THE ASTROPHYSICAL JOURNAL, 546:1038–1054, 2001 January 10

NEUTRINO ASTRONOMY WITH THE MACRO DETECTOR

M. AMBROSIO,[1] R. ANTOLINI,[2] G. AURIEMMA,[3,4] D. BAKARI,[5,6] A. BALDINI,[7] G. C. BARBARINO,[1] B. C. BARISH,[8] G. BATTISTONI,[9,10] R. BELLOTTI,[11] C. BEMPORAD,[7] P. BERNARDINI,[12] H. BILOKON,[9] V. BISI,[13] C. BLOISE,[9] C. BOWER,[14] M. BRIGIDA,[11] S. BUSSINO,[15] F. CAFAGNA,[11] M. CALICCHIO,[11] D. CAMPANA,[1] M. CARBONI,[9] S. CECCHINI,[5,16] F. CEI,[7] V. CHIARELLA,[9] B. C. CHOUDHARY,[8] S. COUTU,[17,18] G. DE CATALDO,[11] H. DEKHISSI,[5,6] C. DE MARZO,[11] I. DE MITRI,[12] J. DERKAOUI,[5,6] M. DE VINCENZI,[15] A. DI CREDICO,[2] O. ERRIQUEZ,[11] C. FAVUZZI,[11] C. FORTI,[9] P. FUSCO,[11] G. GIACOMELLI,[5] G. GIANNINI,[7,19] N. GIGLIETTO,[11] M. GIORGINI,[5] M. GRASSI,[7] L. GRAY,[2] A. GRILLO,[2] F. GUARINO,[1] C. GUSTAVINO,[2] A. HABIG,[20] K. HANSON,[17] R. HEINZ,[14] E. IAROCCI,[9,21] E. KATSAVOUNIDIS,[8] I. KATSAVOUNIDIS,[8] E. KEARNS,[20] H. KIM,[8] S. KYRIAZOPOULOU,[8] E. LAMANNA,[3,22] C. LANE,[23] D. S. LEVIN,[17] P. LIPARI,[3] N. P. LONGLEY,[8,24] M. J. LONGO,[17] F. LOPARCO,[11] F. MAAROUFI,[5,6] G. MANCARELLA,[12] G. MANDRIOLI,[5] S. MANZOOR,[5,25] A. MARGIOTTA,[5] A. MARINI,[9] D. MARTELLO,[12] A. MARZARI-CHIESA,[13] M. N. MAZZIOTTA,[11] D. G. MICHAEL,[8] S. MIKHEYEV,[2,8,26] L. MILLER,[14,27] P. MONACELLI,[28] T. MONTARULI[9,11,] M. MONTENO,[13] S. MUFSON,[14] J. MUSSER,[14] D. NICOLÒ,[7,29] R. NOLTY,[8] C. OKADA,[20] C. ORTH,[20] G. OSTERIA,[1] M. OUCHRIF,[5,6] O. PALAMARA,[2] V. PATERA,[9,21] L. PATRIZII,[5] R. PAZZI,[7] C. W. PECK,[8] L. PERRONE,[12] S. PETRERA,[28] P. PISTILLI,[15] V. POPA,[5,30] A. RAINÒ,[11] J. REYNOLDSON,[2] F. RONGA,[9] C. SATRIANO,[3,4] L. SATTA,[9,21] E. SCAPPARONE,[2] K. SCHOLBERG,[20] A. SCIUBBA,[9,4] P. SERRA,[5] M. SIOLI,[5] M. SITTA,[13] P. SPINELLI,[11] M. SPINETTI,[9] M. SPURIO,[5] R. STEINBERG,[23] J. L. STONE,[20] L. R. SULAK,[20] A. SURDO,[12] G. TARLÈ,[17] V. TOGO,[5] M. VAKILI,[31] E. VILELA,[5] C. W. WALTER,[8,20] AND R. WEBB[31]
(THE MACRO COLLABORATION)

Received 2000 February 26; accepted 2000 August 31

ABSTRACT

High-energy gamma-ray astronomy is now a well-established field, and several sources have been discovered in the region from a few giga–electron volts up to several tera–electron volts. If sources involving hadronic processes exist, the production of photons would be accompanied by neutrinos too. Other possible neutrino sources could be related to the annihilation of weakly interacting, massive particles (WIMPs) at the center of galaxies with black holes. We present the results of a search for pointlike sources using 1100 upward-going muons produced by neutrino interactions in the rock below and inside the Monopole Astrophysics and Cosmic Ray Observatory (MACRO) detector in the underground Gran Sasso Laboratory. These data show no evidence of a possible neutrino pointlike source or of possible correlations between gamma-ray bursts and neutrinos. They have been used to set flux upper limits for candidate pointlike sources which are in the range 10^{-14}–10^{-15} cm^{-2} s^{-1}.

Subject headings: elementary particles — gamma rays: observations

[1] Dipartimento di Fisica dell'Università di Napoli and INFN, 80125 Napoli, Italy.
[2] Laboratori Nazionali del Gran Sasso dell'INFN, 67010 Assergi (L'Aquila), Italy.
[3] Dipartimento di Fisica dell'Università di Roma "La Sapienza" and INFN, 00185 Roma, Italy.
[4] Also Università della Basilicata, 85100 Potenza, Italy.
[5] Dipartimento di Fisica dell'Università di Bologna and INFN, 40126 Bologna, Italy.
[6] L.P.T.P., Faculty of Sciences, University Mohamed I, B.P. 524 Oujda, Morocco.
[7] Dipartimento di Fisica dell'Università di Pisa and INFN, 56010 Pisa, Italy.
[8] California Institute of Technology, Pasadena, CA 91125.
[9] Laboratori Nazionali di Frascati dell'INFN, 00044 Frascati (Roma), Italy.
[10] Also INFN Milano, 20133 Milano, Italy.
[11] Dipartimento di Fisica dell'Università di Bari and INFN, 70126 Bari, Italy.
[12] Dipartimento di Fisica dell'Università di Lecce and INFN, 73100 Lecce, Italy.
[13] Dipartimento di Fisica Sperimentale dell'Università di Torino and INFN, 10125 Torino, Italy.
[14] Departments of Physics and of Astronomy, Indiana University, Bloomington, IN 47405.
[15] Dipartimento di Fisica dell'Università di Roma Tre and INFN Sezione Roma Tre, 00146 Roma, Italy.
[16] Also Istituto TESRE/CNR, 40129 Bologna, Italy.
[17] Department of Physics, University of Michigan, Ann Arbor, MI 48109.
[18] Also Department of Physics, Pennsylvania State University, University Park, PA 16801.
[19] Also Università di Trieste and INFN, 34100 Trieste, Italy.
[20] Physics Department, Boston University, Boston, MA 02215.
[21] Also Dipartimento di Energetica, Università di Roma, 00185 Roma, Italy.
[22] Also Dipartimento di Fisica dell'Università della Calabria, Rende (Cosenza), Italy.
[23] Department of Physics, Drexel University, Philadelphia, PA 19104.
[24] Colorado College, Colorado Springs, CO 80903.
[25] Also RPD, PINSTECH, P.O. Nilore, Islamabad, Pakistan.
[26] Also Institute for Nuclear Research, Russian Academy of Science, 117312 Moscow, Russia.
[27] Also Department of Physics, James Madison University, Harrisonburg, VA 22807.
[28] Dipartimento di Fisica dell'Università dell'Aquila and INFN, 67100 L'Aquila, Italy.
[29] Also Scuola Normale Superiore di Pisa, 56010 Pisa, Italy.
[30] Also Institute for Space Sciences, 76900 Bucharest, Romania.
[31] Physics Department, Texas A&M University, College Station, TX 77843.

1. MOTIVATIONS FOR NEUTRINO ASTRONOMY

Neutral particles, such as photons and neutrinos, and protons of energies $\gtrsim 10^7$ TeV are not deflected by magnetic fields during their propagation, and they point back to their sources. Hence they are probes to study our universe. Photons are currently the main observation channel of our universe, and the field of gamma-ray astronomy is now well established. On the other hand, the universe becomes opaque to protons with energies above $\sim 5 \times 10^{19}$ eV at distances of ~ 30 Mpc due to photopion production with the cosmic microwave background radiation (CMBR; Greisen 1966; Zatseptin & Kuz'min 1966).

The idea of using neutrinos as probes of the deep universe was introduced in the 1960s (Greisen 1960; Bahcall & Frautschi 1964). Neutrinos are weakly interacting particles and are therefore much less absorbed than gamma rays and protons at the source and during propagation, so they can bring information on the deep interior of sources and on the far universe. Some examples of detection of cosmic neutrinos already exist: solar neutrinos (from 0.1 MeV up to ~ 10 MeV; Davis, Harmer, & Hoffman 1968) and neutrinos from SN 1987A (from ~ 10 MeV up to ~ 50 MeV; Hirata et al. 1987; Bionta et al. 1987). Nevertheless, neutrinos of astrophysical origin with energies larger than 100 MeV have not yet been observed. This observation would open the new field of high-energy neutrino astronomy complementary to gamma-ray astronomy.

Satellites, ground-based imaging Cherenkov telescopes, and extensive air shower arrays are currently investigating the universe using photons as probes (Jackson, Gove, & Lüth 1993). Ground-based experiments have detected a smaller number of sources so far than space experiments, such as EGRET. The EGRET detector on board the *Compton Gamma Ray Observatory* (*CGRO*) satellite has thus far furnished the largest amount of information on sources up to ~ 30 GeV. The recent third EGRET catalog,[32] covering the observations made from 1991 to 1995, contains 271 sources observed with energies greater than 100 MeV. Among them, there are five pulsars, one probable radio galaxy (Cen A), 66 high-confidence identifications of blazars (BL Lac objects and radio quasars), 27 lower confidence potential blazar identifications, and a large number of identified supernova remnants (SNRs), and also 170 sources not yet identified firmly with known objects.

Satellite-based detectors are providing observations on gamma-ray bursts (GRBs) capable of solving the mystery concerning their nature. The BATSE experiment[33] on the *CGRO* satellite has now detected more than 2500 gamma-ray bursts, and the Italian-Dutch *BeppoSAX* satellite (Frontera 1997) is providing breakthroughs thanks to the precise measurement of the position of the bursts.

Cherenkov telescopes at ground level, such as the Whipple Observatory, the High-Energy Gamma-Ray Array (HEGRA), the Collaboration between Australia and Nippon for a Gamma-Ray Observatory in the Outback (CANGAROO), and the University of Durham Mark 6 telescopes, have so far detected eight sources emitting gamma-rays well above 300 GeV: the supernova remnants Crab (Lang et al. 1990), Vela Pulsar (at a distance of only ~ 500 pc; Yoshikoshi et al. 1997), and SN 1006 (Tanimori et al. 1998); the extragalactic BL Lac objects (highly variable active galactic nuclei) Mrk 421 ($z = 0.031$; Punch et al. 1992; Petry et al. 1997), Mrk 501 ($z < 0.034$; Quinn et al. 1996), and PKS $2155-304$ ($z = 0.116$; Chadwick et al. 1999); and the pulsars PSR $1706-44$ (Kifune et al. 1995) and PSR $1259-63$ (Sako et al. 1997).

The discovery of tera–electron volt gamma rays emitted from the eight sources given above shows the possibility of alternate mechanisms of production to electron energy loss ones and the possible existence of beam dump sources (see § 2) producing photons and high-energy neutrinos from pion decay. Nevertheless, "a few tera–electron volts" are not high enough energies to exclude a synchrotron radiation production mechanism, which could instead be completely excluded for sources of energies above 100 TeV. Those energies cannot be explained by electron energy losses because electron acceleration is limited by the intense synchrotron radiation produced in the ambient magnetic fields.

A different kind of neutrino production from astrophysical sources has been suggested by Gondolo & Silk (1999). If cold dark matter exists in the Galactic center, it can be accreted by the black hole that probably is there and redistributed by the black hole into a cusp (called a "central spike"). If dark matter is made of the supersymmetric neutralino, its annihilation rate in the spike is strongly increased as it depends on the square of the matter density. Neutrinos can escape and produce relevant fluxes. For the neutralino, the muon fluxes are very high in the case of the presence of a central spike at the level of 10^{-15}–10^{-14} cm^{-2} s^{-1} for $m_\chi \gtrsim 50$ GeV, which would produce in a detector like the Monopole Astrophysics and Cosmic Ray Observatory (MACRO) $\sim$1–20 events yr^{-1} 1000 m^{-2}.

During the 1970s and 1980s, the first generation underground detectors of surface ~ 100 m^2 produced results in searches for astrophysical sources of neutrinos. Previous results in the search for pointlike sources have been published by the Kolar Gold Field experiment (Adarkar et al. 1991, 1995) and by the water Cherenkov detectors Irvine-Michigan-Brookhaven (IMB; Svoboda 1987; Becker-Szendy 1995a, 1995b) and Kamiokande (Oyama et al. 1989). Preliminary results of other experiments (Baksan [Boliev et al. 1995] and the Antarctic Muon and Neutrino Detector Array [AMANDA; John 1999]) have been presented at conferences. MACRO has been detecting muon neutrinos since 1989, when it was still under construction. We present here the results of the search for astrophysical neutrino sources with MACRO during the period 1989 March to 1999 September.

2. NEUTRINO ASTRONOMY

Astrophysical neutrinos can be produced in the interactions of protons accelerated by compact sources with a target around the source (gas of matter or photons). This is the most plausible model for a neutrino source, the so-called beam dump model (Berezinsky, Castagnoli, & Galeotti 1985; Gaisser, Halzen, & Stanev 1995). The acceleration process requires the presence of a strong magnetic field with sufficient local gas to act as a beam dump. The column density of the gas in the source is assumed to be larger than the nuclear depth ($x_N \sim 70$ g cm^{-2}) but smaller than the neutrino absorption depth due mainly to νN inter-

[32] Hartman, R. C., et al. 1998, available at the URL ftp://gamma.gsfc.nasa.gov/pub/THIRD_CATALOG.

[33] Paciesas, W. S., et al. 1999, available at the URL http://gammaray.msfc.nasa.gov/batse.

actions [$x_\nu \sim 3 \times 10^{12}(100\ \mathrm{GeV}/E_\nu\ \mathrm{g\ cm^{-2}})$ and $x_{\bar{\nu}} \sim 6 \times 10^{12}(100\ \mathrm{GeV}/E_{\bar{\nu}}\ \mathrm{g\ cm^{-2}})$; Berezinsky et al. 1985]. The chain of reactions is

$$p + N(\gamma) \rightarrow \pi^0 \quad + \quad \pi^\pm + \cdots$$
$$\searrow \gamma + \gamma \quad \searrow \mu^\pm + \nu_\mu(\bar{\nu}_\mu)$$
$$\searrow e^+ + \nu_e + \bar{\nu}_\mu \ (e^- + \bar{\nu}_e + \nu_\mu) \ . \quad (1)$$

Neutral pions produce the observed photons; the production of charged pions and kaons, which can decay, producing neutrinos and muons, is expected from the same chain. Moreover, muons decay too. The result is neutrinos and antineutrinos of electron and muon flavors. Neglecting the photon absorption effect, which is subject to very large uncertainties, the neutrino flux has at least the same spectral shape and intensity with respect to the gamma-ray flux; hence very low neutrino event rates are expected due to the small neutrino cross section. The presence of $\gtrsim 100$ TeV gamma-ray sources should guarantee the existence of neutrino sources, but no reliable information can be drawn on neutrino fluxes from gamma-ray ones because they are subject to nonnegligible absorption.

Cosmic accelerators produce a power-law spectrum,

$$\frac{d\phi}{dE_\nu} \propto E^{-(\gamma+1)} , \quad (2)$$

with $\gamma \sim 1$–1.5. The first-order Fermi acceleration mechanism in strong shock waves has the attractive feature of resulting in this kind of power-law spectrum (Longair 1997), and it predicts a spectral index $\gamma \sim 1$. Hence, neutrinos produced by cosmic rays at their acceleration sites should follow the hard spectrum of their parents in equation (2).

For sources in which the p-γ scattering dominates, such as in active galactic nuclei (AGNs), the resulting neutrino spectrum reproduces the spectrum of the parent accelerated nucleons (as in p-p scattering) at neutrino energies $E_\nu \gg m_p^2/\omega_0$, where ω_0 is the energy at which the photon spectrum has a maximum (Berezinsky & Gazizov 1993). At energies lower than this threshold, the neutrino differential spectrum is almost constant with energy.

The primary cosmic rays impinging on the Earth's atmosphere have a slightly steeper spectrum than the ones resulting from a cosmic accelerator because of the energy dependence of the cosmic-ray diffusion out of the Galaxy (Gaisser et al. 1995). Hence, the spectrum of neutrinos produced in the cascades induced by primary cosmic-ray interactions with the atmospheric nuclei is steeper than the one from a cosmic accelerator. Atmospheric muon and electron neutrinos originate from decay of pions, kaons, and muons. At neutrino energies $\lesssim 10$ GeV, since all parent mesons of atmospheric neutrinos decay, the atmospheric neutrino spectrum follows the spectrum of the parent cosmic rays [$(d\phi_\nu/dE)_{\mathrm{atm}} \propto E^{-2.7}$]. For higher energies, since the path length in the atmosphere is not large enough to allow the decay of all pions and kaons, interactions of mesons begin to dominate, and the atmospheric neutrino spectrum becomes steeper [$(d\phi_\nu/dE)_{\mathrm{atm}} \propto E^{-3.7}$ for $E_\nu \gtrsim 100$ GeV] due to the change of the spectral index of the meson spectra. These neutrinos originating in the Earth's atmosphere are a background for the search for astrophysical neutrinos. Due to their steeper spectrum with respect to neutrinos produced by cosmic accelerators, the signal-to-noise ratio becomes larger at increasing energies, and above some tens of tera–electron volts, the neutrinos from sources start to dominate.

The search presented here uses only the direction information of the neutrinos. Since MACRO angular resolution is very good and since the energy range of neutrinos is above 1 GeV, we can look around source directions in narrow angular cones, hence minimizing the atmospheric neutrino background. For many of the sources considered in this search, we are not yet limited by the atmospheric neutrino background as we measure no events in the cone. For other sources we see some events in the cone that are compatible with the number of events expected by the atmospheric neutrino background.

Other searches could maximize the signal-to-noise ratio using the energy information on the detected particle and looking to the diffuse neutrino events from the whole sky. This was done by the Frejus experiment (Rhode et al. 1996), and some results have been recently presented by the Baikal Collaboration (Balkanov et al. 2000). Preliminary MACRO results were presented elsewhere (Corona 1995) and will be the subject of a future paper.

2.1. *Candidate Sources and Expected Rates*

High-energy neutrinos are expected to be emitted from a wide class of possible celestial objects, which can be divided into two wide subclasses: galactic sources and extragalactic sources (Gaisser et al. 1995).

Galactic sources are energetic systems, such as binary systems and supernova remnants, in which cosmic rays are accelerated and interact with matter (mainly protons). The most interesting sources are SNRs, which are the most likely sources to be observed by a detector of the MACRO size. In such systems, the target is the material of the expanding shell, and the accelerating mechanism is originated by the intense magnetic field of the pulsar. There are, however, possibilities of having neutrino emissions originate by acceleration at the supernova blast waves and therefore neutrino emissions even without pulsars. The neutrino emission should be in an active time of up to a few years. Of course, the disadvantage of galactic supernovae as neutrino emitters is that their rate is low (of the order of 1 per 30 yr). According to detailed calculations made for several historical supernova (Gaisser 1996), the most intense source should be the supernova remnant Vela Pulsar, with a rate of upward-going muons induced by neutrinos in the rock surrounding a detector of the order 0.1 event $\mathrm{yr^{-1}}$ 1000 $\mathrm{m^{-2}}$ for $E_\mu > 1$ GeV. Another model for young SNRs with a pulsar having a high magnetic field and short period (~ 5 ms) is suggested in Protheroe, Bednarek, & Luo (1998): for a beaming solid angle of neutrino emission of 1 sr, about 5 events $\mathrm{yr^{-1}}$ are expected in 1000 $\mathrm{m^2}$ for $E_\nu \geq 100$ GeV after 0.1 yr from an explosion at a distance of 10 kpc.

Possible extragalactic sources are active galactic nuclei and gamma-ray bursters. For these sources the dominant mechanism for producing neutrinos is accelerated protons interacting on ambient photons. Possible alternative mechanisms are the so-called top-down models (Sigl et al. 1997).

Active galactic nuclei, being among the most luminous objects in the universe, with luminosities ranging from 10^{42} to 10^{48} ergs $\mathrm{s^{-1}}$, have been recognized for a long time as promising possible sources of neutrinos. Present models assume that they consist of a central engine (massive black hole) with an accretion disk and jets (Gaisser et al. 1995).

Accretion onto the central black hole provides the total power. Two possible sources of high-energy neutrino fluxes within AGNs have been suggested. The first is associated with the central engine and the second with the production in jets associated with several blazars (radio-loud AGNs in which the beam intersects the observer line of sight). AGNs could emit neutrinos up to $\sim 10^{10}$ GeV.

Even considering the highest luminosities and the presence of jets, single AGNs are difficult to detect. Jets carry about 10% of the AGN luminosity, and AGNs may appear brighter because of the motion of the emitting matter toward the observer (for an observer looking along the jet axis, $E_{\rm obs} = \Gamma E_{\rm jet}$ and $L_{\rm obs} = \Gamma^4 L_{\rm jet}$, where Γ is the Lorentz factor). Expected event rates for blazars are of the order of 10^{-2}–10^{-1} 1000 m^{-2} yr^{-1} for $\Gamma = 10$–10^2 and $E_\nu > 1$ TeV (Halzen 2000).

Stecker et al. (1991) suggested the possibility of integrating the neutrino flux from single generic AGNs to obtain a diffuse flux from all cosmological AGNs. Various models have been suggested (Stecker et al. 1991; Szabo & Protheroe 1994),[34] and the event rates in upward-going muons vary between $\sim 10^{-1}$–10 1000 m^{-2} yr^{-1} for $E_\nu > 1$ TeV.

Gamma-ray bursters are considered to be promising sources of high-energy neutrinos. They yield transient events originating beyond the solar system, with typical durations of 10^{-2}–10^3 s. The BATSE experiment[33] has now collected more than 2500 events, which appear isotropically distributed. This feature suggests that they are located at cosmological distances. The recent observations by *BeppoSAX* of GRB 970228 have allowed the precise measurement of the position, which led to the identification of a fading optical counterpart (Costa et al. 1997) for the first time. The direct measurement, immediately after, of the redshift in the optical afterglow at $z = 0.835$ for GRB 970508 (Metzger et al. 1997) and other identifications of the distances of GRBs have given support to the cosmological origin hypothesis. These observations make GRBs the most luminous objects observed in our universe, with emitted energies $\gtrsim 10^{51}$ ergs and a spectrum peaked between 100 keV and 1 MeV.

One of the most plausible models is the "fireball model," which solves the compactness problem by introducing a beamed relativistic motion with $\Gamma \gtrsim 100$ of an expanding fireball (Piran 1999). The question of the energy of the engine of GRBs, which is strictly connected to that of beaming, is still under discussion. Evidence for beaming are a break and a steepening of the spectrum. They have been found in spectra of some bursts, e.g., GRB 980519 and GRB 990123. In the case of GRB 990123, at $z = 1.6$ for isotropic emission the emitted energy would be the highest ever observed (2×10^{54} ergs), while if there is a beam, the emitted energy would be reduced to $\sim 10^{52}$ ergs due to the Lorentz factor.

Several authors have suggested a possible correlation between gamma-ray bursters and emissions of high-energy neutrinos produced by accelerated protons on photons (Halzen & Jaczo 1996; Waxman & Bahcall 1997; Rachen & Meszaros 1998; Vietri 1998). Expected rates could be up to 10^6 muon-induced events in a 1000 m^2 detector for muon energies above ~ 30 TeV for emissions lasting less than 1 s (Halzen & Jaczo 1996). In other scenarios, such as for fireballs, rates are of the order of $\sim 10^{-3}$ upward-going muons in a 1000 m^2–size detector for a burst at a distance of 100 Mpc producing 0.4×10^{51} ergs in 10^{14} eV neutrinos (Waxman & Bahcall 1999). Considering a rate of 10^3 bursts yr^{-1} over 4π sr, averaging over burst distances and energies, $\sim 2 \times 10^{-2}$ upward-going muons are expected in 1000 m^2 yr^{-1} for 4π sr (Waxman & Bahcall 1997). It is important to consider that the uncertainty in the Lorentz factor Γ produces high variations in the expected rates: the higher the Γ, the larger the luminosity at the observer ($L_{\rm obs} \sim \Gamma^4 L_{\rm jet}$), but the smaller the rates of events because the actual photon target density in the fireball is diluted by large Lorentz factors (the fraction of total energy going into pion production in the source and hence into neutrinos varies approximately as Γ^{-4} [Halzen & Hooper 1999]).

According to Waxman & Bahcall (1999, hereafter WB), an energy-independent upper bound on diffuse fluxes of neutrinos with $E_\nu \gtrsim 10^{14}$ eV produced by photomeson or p-p interactions in sources from which protons can escape can be estimated at the level of $E_\nu^2 \phi_\nu < 2 \times 10^{-8}$ GeV cm^{-2} s^{-1} sr^{-1}. This bound relies on the flux measurement of extremely high energy cosmic rays in extensive air showers, which are assumed to be of extragalactic origin. Their limit would exclude most of the present models of neutrino production in AGNs, which are commonly normalized to the extragalactic mega–electron volt to giga–electron volt gamma-ray background. Contrary to WB, Mannheim, Protheroe, & Rachen (1998) find an energy-dependent upper limit that agrees within a factor of 2 with WB in the limited range of $E_\nu \sim 10^{16-18}$ eV, while at other energies the neutrino flux is mainly limited by its contribution to extragalactic gamma-ray background, which is at a level of about 2 orders of magnitude higher than the WB limit.

3. THE MACRO DETECTOR AND THE DATA SELECTION

In the range of energies from several giga–electron volts to several tera–electron volts, the neutrinos produced by astrophysical sources can be detected in underground detectors as upward-going muons produced by neutrino charged current (CC) interactions in the rock surrounding the detector. Neutrino events can be discriminated from among the background of atmospheric muons that are larger by many orders of magnitude ($\sim 5 \times 10^5$ at MACRO depth) by recognizing that they travel from the bottom to the top of the apparatus after having crossed the Earth. Neutrino detection is experimentally much more difficult than the gamma-ray one: because of the low neutrino interaction cross section, it requires very large detectors.

The MACRO detector, shown in Figure 1 and described in detail in Ahlen et al. (1993), is located in Hall B of the Gran Sasso underground laboratory at a minimum rock depth of 3150 hg cm^{-2} and an average rock depth of 3700 hg cm^{-2}. The detector, 76.6 m long, 12 m wide, and 9.3 m high, is divided longitudinally into six similar supermodules and vertically into a lower part (4.8 m high) and an upper part (4.5 m high).

The active detectors include 14 horizontal and 12 vertical planes of 3 cm–wide limited streamer tubes for particle tracking and liquid scintillation counters for fast timing. In the lower part, the eight inner planes of limited streamer tubes are separated by passive absorbers (iron and rock, ~ 50 g cm^{-2}) in order to set a minimum threshold of ~ 1

[34] Most of the Szabo & Protheroe (1994) models are excluded by the Frejus limit (Rhode et al. 1996).

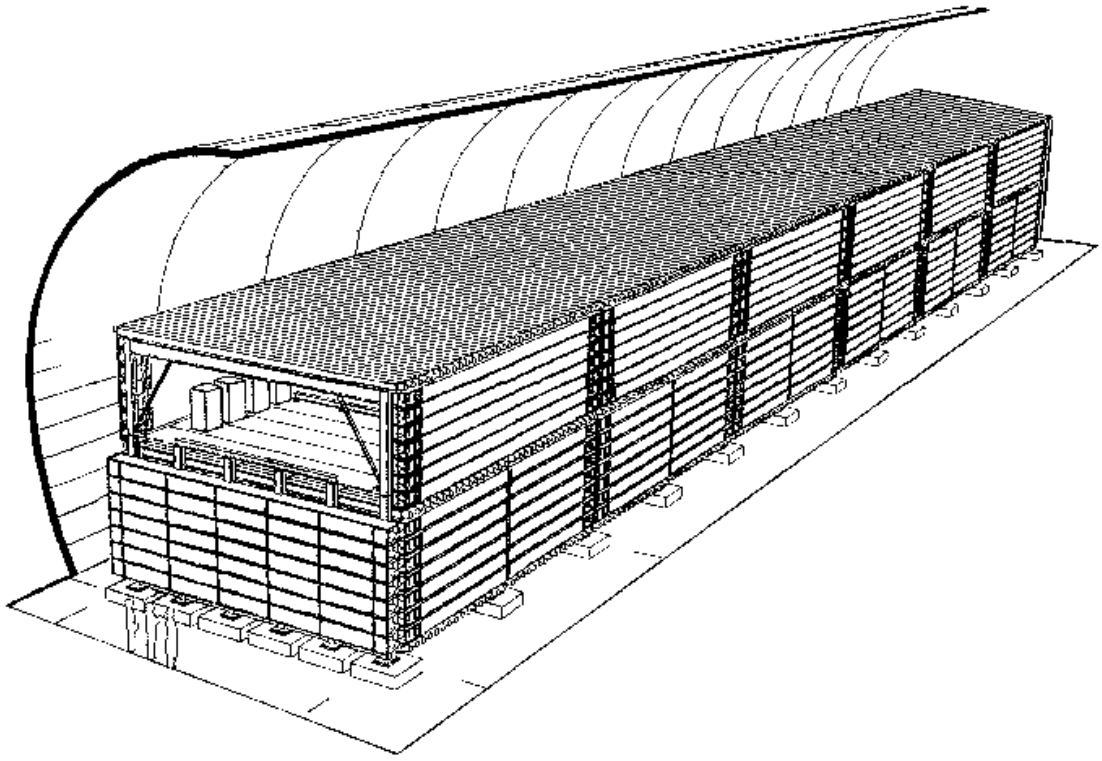

FIG. 1.—Layout of the MACRO detector

GeV for vertical muons crossing the detector. The upper part of the detector is an open volume containing electronics and other equipment. The horizontal streamer tube planes are instrumented with external 3 cm pick-up strips at an angle of 26°.5 with respect to the streamer tube wires, providing stereo readout of the detector hits. The transit time of particles through the detector is measured by the time of flight (TOF) technique using scintillation counters. The mean time at which signals are observed at the two ends of each counter is measured, and the difference in the measured mean time between counters located in different planes gives the TOF. The time resolution of the scintillation counter system is about 500 ps.

In order to achieve the largest reconstruction efficiency for all directions, three algorithms for muon tracking are used in this analysis. The first kind of tracking is for events with aligned hits in at least four horizontal planes, the second is for events with at least two horizontal planes in coincidence with at least three vertical planes, and the third is for events having at least three vertical planes in coincidence with two scintillation counters (this tracking is useful for almost horizontal tracks).

The angular resolution depends on the wire and strip cluster widths and on the track length. The average error on the slopes of tracks are 0°.14 for the wires and 0°.29 for the strips (Ahlen et al. 1993). Our pointing capabilities for point sources have been checked with the observation of the Moon-shadowing effect using atmospheric down-going muons (Ambrosio et al. 1999).

The data used for the upward-going muon search belong to three running periods with different apparatus configurations: 26 events were detected with the lower half of the first supermodule from 1989 March to 1991 November (about 1/12 of the full acceptance, with an effective acquisition time or "live time" of 1.38 yr, efficiencies included), 55 with the full lower half of the detector (about 60% of the full acceptance) from 1992 December to 1993 June (0.41 yr, efficiencies included), and starting from 1994 April, the apparatus has been running in the final configuration. From 1994 April until 1999 September, we have measured 1000 events with the full detector (4.41 yr, including efficiencies). We also consider events which were measured during periods when the detector acceptance was changing with time due to construction work (19 events in 0.2 yr during 1992).

The selection of upward-going muons using the TOF technique has been described in detail in Ambrosio et al. (1995, 1998a). The velocity and direction of muons are determined from the TOF between at least two scintillation layers combined with the path length of a track reconstructed using the streamers. Taking as a reference the upper counter which measures the time T_1, the time of flight $\Delta T = T_1 - T_2$ is positive if the muon travels downward and negative if it travels upward. Figure 2 shows the $1/\beta = c\Delta T/L$ (L is the track length and c the speed of light) distribution for the entire data set. In this convention, muons going down through the detector have $1/\beta \sim 1$, while muons going upward have $1/\beta \sim -1$. Several cuts are imposed to remove backgrounds caused by radioactivity in coincidence with muons and multiple muons. The main cut requires that the position of a muon crossing a scintillator agree within 70 cm (140 cm for slanted tracks with $\cos\theta \leq 0.2$) with the position along the counter determined by the more precise streamer system. Other cuts apply only to events which cross two scintillator planes only. These cuts tend to remove high-multiplicity events because when more than one track crosses the same scintillator box, the reconstructed time of the event is wrong. Events which cross more than two scin-

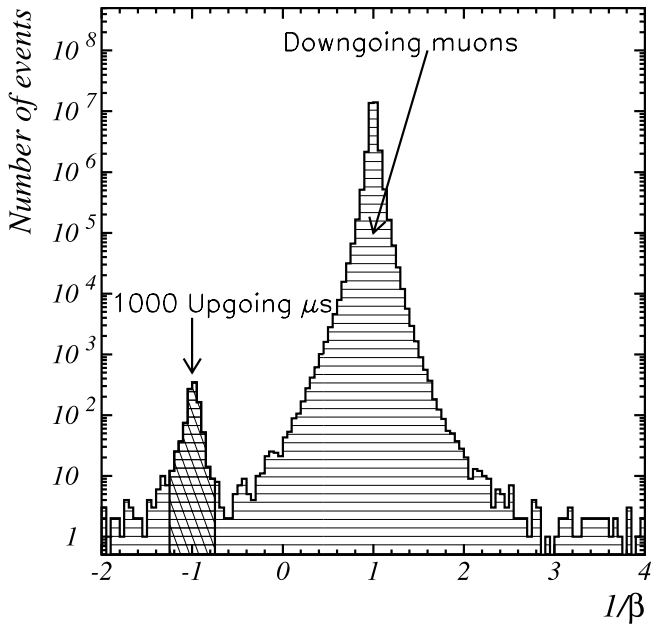

FIG. 2.—The $1/\beta$ distribution for the muon data sample collected with the full detector. The number of down-going muons is $\sim 33.8 \times 10^6$.

tillator planes (about 50% of the total) have a more reliable time determination thanks to the possibility of evaluating the velocity of the particle from a linear fit of times as a function of the height of the scintillator counters. In this case, the only cut then is on the quality of the fit ($\chi^2 \leq 10$).

Events in the range $-1.25 < 1/\beta < -0.75$ are defined to be upward-going muon events. There are 1100 events that satisfy this definition summed over all running periods.[35] One event is shown in Figure 3. In order to maximize the acceptance for this search, we do not require that a minimum amount of material be crossed by the muon track as was done in selecting the sample used for the neutrino oscillation analysis (Ambrosio et al.1995, 1998a). Without this requirement we introduce some background due to large-angle pions produced by down-going muons (Ambrosio et al. 1998b). We also include events with an interaction vertex inside the lower half of the detector. All of these data can be used for the pointlike astrophysical source search since the benefit of a greater exposure for setting flux limits offsets the slight increase of the background and of the systematic error in the acceptance. Moreover, one notices that for neutrino oscillation studies, upward-going muons are mostly signal and background rejection is very critical, while for neutrino astronomy, upward-going muons are mostly background due to atmospheric neutrinos and background rejection is less critical.

[35] The equatorial coordinates and UT times of detection of the 1100 events are available at the URL http://wsgs02.lngs.infn.it:8000/macro/neutrinos.

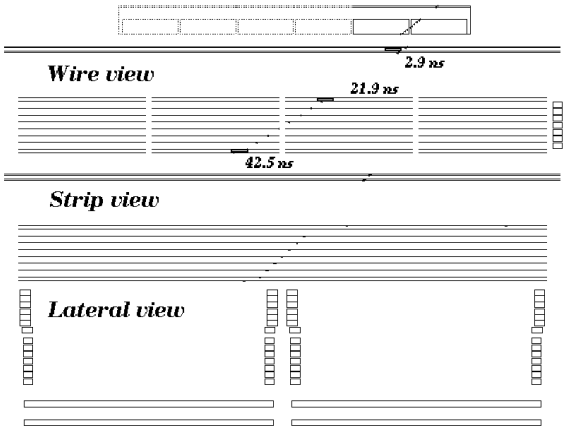

FIG. 3.—One upward-going muon produced by a neutrino interaction in the rock below the MACRO detector. The wire, strip, and lateral views are shown and the times in nanoseconds are indicated near the scintillator counters hit by the track. The first hit counter corresponds to the larger time.

4. NEUTRINO SIGNAL IN UPWARD-GOING MUONS

Muon neutrinos are detected as upward-going muons through CC interactions:

$$\nu_\mu(\bar{\nu}_\mu) + N \rightarrow \mu^-(\mu^+) + X \, . \quad (3)$$

The probability that a neutrino (or antineutrino) with energy E_ν interacts in the rock below the detector and gives rise to a muon that crosses the apparatus with energy $E_\mu \geq E_\mu^{\rm th}$ ($E_\mu^{\rm th}$ is the energy threshold of the apparatus) is

$$P_\nu(E_\nu, E_\mu^{\rm th}) = N_{\rm A} \int_0^{E_\nu} dE'_\mu \, \frac{d\sigma_\nu}{dE'_\mu}(E'_\mu, E_\nu) R_{\rm eff}(E'_\mu, E_\mu^{\rm th}) \, , \quad (4)$$

where $N_{\rm A}$ is Avogadro's number. This probability is a convolution of the ν cross sections and of the muon effective range $R_{\rm eff}(E_\mu, E_\mu^{\rm th})$ described below; the computed probability is shown in Figure 4 and some values are given in Table 1. The trend of the probability at energies $\lesssim 1$ TeV reflects the cross section linear rise with neutrino energy ($\sigma_\nu \propto E_\nu$) and that of the muon range ($R_{\rm eff} \propto E_\mu$), while at higher energies it reflects the damping effect of the propagator ($\sigma_\nu \propto E_\nu^{0.4}$ for $E_\nu \gtrsim 10^3$ TeV) and the logarithmic rise of the muon range with its energy.

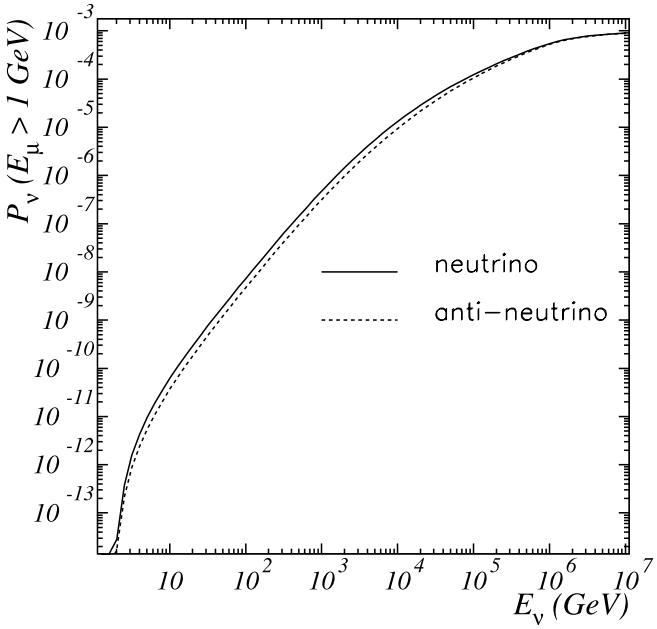

FIG. 4.—Probability that a ν with E_ν crossing the detector produces a muon above threshold. *Solid line*, neutrino; *dotted line*, antineutrino.

TABLE 1

VALUES OF THE PROBABILITY[a] OF A NEUTRINO OR ANTINEUTRINO PRODUCING A MUON WITH ENERGY LARGER THAN THE ENERGY THRESHOLD OF 1 GeV AS A FUNCTION OF THE NEUTRINO ENERGY

E_ν (GeV)	$P_{\nu\to\mu^-}$	$P_{\bar{\nu}\to\mu^+}$
10.....	8.15×10^{-11}	4.88×10^{-11}
10^2.....	9.05×10^{-9}	5.87×10^{-9}
10^3.....	5.79×10^{-7}	3.86×10^{-7}
10^4.....	1.52×10^{-5}	1.09×10^{-5}
10^5.....	1.35×10^{-4}	1.17×10^{-4}

[a] Given in eq. (4).

It is relevant to notice that, thanks to the recent Hadron Electron Ring Accelerator (HERA) measurements (Wolf 1995), our knowledge of the high-energy deep inelastic neutrino cross section has improved significantly. There is good agreement between various sets of parton functions that provide confident predictions of the cross sections up to 10^6 GeV (Gandhi et al. 1996, 1998). For the calculation of the probability shown in Figure 4, we have used the CTEQ3-DIS (Lai et al. 1995) parton functions, available in the PDFLIB CERN library (Plothow-Besch 1993), which have been considered by Gandhi et al. (1996, 1998) and are in good agreement with the more recent CTEQ4-DIS.

The technique of detecting upward-going muons generated in the rock surrounding a detector has the advantage of increasing the effective detector mass, which in fact is a convolution of the detector area and of the muon range in the rock. The gain increases with energy: for example, for tera–electron volt muons, the range is of the order of 1 km. The effective muon range is given by the probability that a muon with energy E_μ survives with energy above threshold after propagating a distance X:

$$R_{\rm eff}(E_\mu, E_\mu^{\rm th}) = \int_0^\infty dX\, P_{\rm surv}(E_\mu, E_\mu^{\rm th}, X)\,, \tag{5}$$

where the integral is evaluated from the μ energy losses. We have used the energy loss calculation by Lohmann, Kopp, & Voss (1985), using standard rock for muon energies up to 10^5 GeV. For higher energies we use the approximate formula

$$\frac{dE_\mu}{dX} = \alpha + \beta E_\mu\,, \tag{6}$$

where $\alpha \sim 2.0$ MeV g^{-1} cm^2 takes into account the continuous ionization losses and $\beta \sim 3.9 \times 10^{-6}$ g^{-1} cm^2 takes into account the stochastic losses due to bremsstrahlung, pair production, and nuclear interactions.

The flux of neutrino-induced muons detected by an apparatus for a source of declination δ and for a neutrino spectrum $\Phi_\nu(E_\nu) \propto E^{-\gamma}$ is

$$\Phi_\mu(E_\mu^{\rm th}, E_\nu, \delta) = N_{\rm A} \int_{E_\mu^{\rm th}}^{E_\mu^{\rm max}} \frac{d\sigma_\nu}{dE'_\mu}(E'_\mu, E_\nu) \times R_{\rm eff}(E'_\mu, E_\mu^{\rm th}) {\rm Area}(E'_\mu, \delta) \Phi_\nu(E_\nu) dE'_\mu\,. \tag{7}$$

The effective area of the detector Area(E'_μ, δ), averaged over 24 hr, depends on source declination and on muon energy. In the low-energy region, the effective area increases with increasing muon energy because not all muons are detected, depending on their track length in the detector. At higher energies (in MACRO for $E_\mu \gtrsim 3$ GeV) it reaches a plateau when all muons from all directions have enough energy to be detected. At very high energies the effective area can decrease due to electromagnetic showers. As a matter of fact, the efficiency of the analysis cuts can decrease due to high track multiplicities for high-energy events. Moreover, the presence of showers could lead to a bad reconstruction of the neutrino-induced muon with another track of the shower. From Monte Carlo studies, the MACRO average effective area begins to decrease for $E_\mu \gtrsim 1$ TeV, and it is about 20% (42%) lower at 10 TeV (100 TeV) with respect to 10 GeV. The average area as a function of declination for various energies is shown in Figure 5. It has been obtained using the detector simulation based on GEANT (Brun et al. 1987) but modified to properly treat the stochastic muon energy losses above 10 TeV (Bottai & Perrone 2000). To obtain large Monte Carlo statistics we have used "beams" of monoenergetic muons intercepting isotropically from the lower hemisphere a volume containing MACRO and more than 2 m of the surrounding rock (to evaluate the effect of electromagnetic showers induced by high-energy muons). For each beam energy, we have simulated about 10^5 muons.

Due to the increasing value of the ν cross section, at high energies neutrinos are "absorbed" by the large amount of material they cross through the Earth. Neutrino absorption in the Earth can be taken into account by introducing in the integral in equation (7) the exponential factor

$$e^{-N_A \sigma_\nu(E) X(\cos\theta)}\,, \tag{8}$$

which depends on $X(\cos\theta)$, the quantity of matter crossed by the incident neutrino in the Earth, and hence on its zenith angle. The differential number of neutrinos that produce detectable muons as a function of the neutrino energy (response curves) for a source of differential spectral

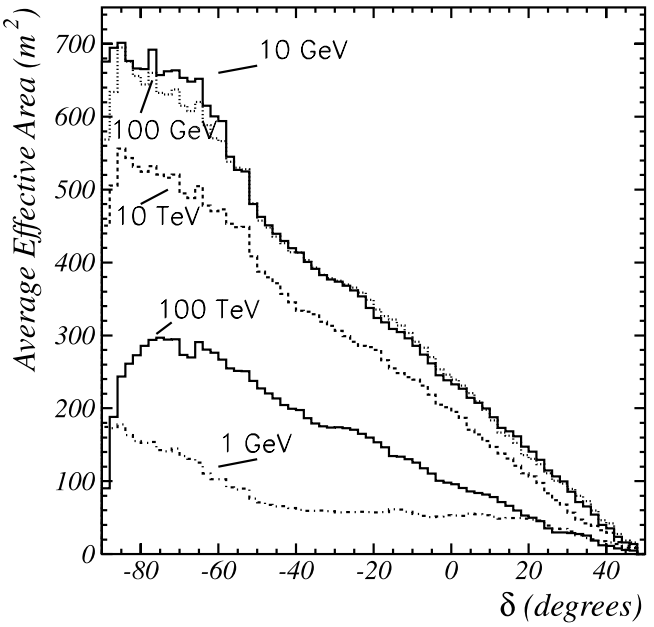

FIG. 5.—MACRO average effective area as a function of declination for various muon energies. From top to bottom lines: 10 GeV (*solid line*), 100 GeV (*dotted line*), 10 TeV (*dashed line*), 100 TeV (*solid line*), and 1 GeV (*dot-dashed line*).

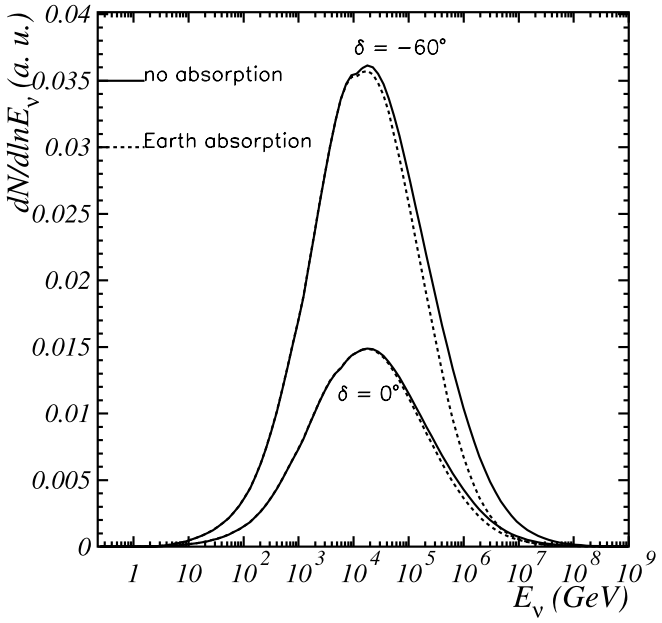

FIG. 6.—MACRO response curve, which is the differential rate of neutrinos that induce detectable muons as a function of the neutrino energy, for two sources at declinations $-60°$ and 0°. Solid (dotted) lines do not (do) include Earth absorption. The normalization of the neutrino fluxes is arbitrary.

index $\gamma = 2.1$ at two different declinations with and without absorption in the Earth is shown in Figure 6. The median neutrino energy is about 15 TeV, while for the atmospheric neutrinos it is between 50 and 100 GeV (Ambrosio 1998a). It is noticeable how the absorption becomes negligible for sources seen near the horizon ($\delta \sim 0°$). In Figure 7 the same response curves are shown for three spectral indices. In these plots, the normalization of the neutrino fluxes is arbitrary. From Figures 6 and 7 we see that MACRO is mostly sensitive in the neutrino energy region between 10^3 and 10^5 GeV to neutrino fluxes from sources with spectral indices between 2.1 and 2.3. For larger values of the spectral index, the maximum of the response curve moves toward lower energies.

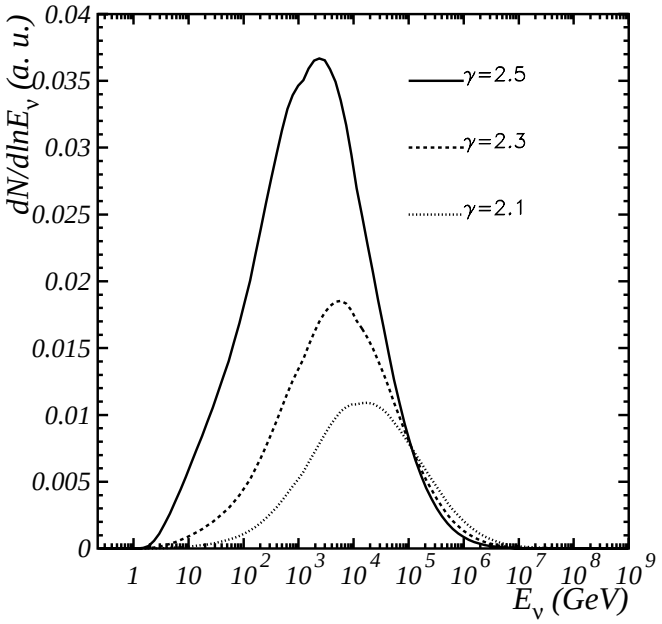

FIG. 7.—MACRO response curves for spectral indices ($\gamma = 2.1$, 2.3, 2.5) for a source at declination $-60°$. Earth absorption is included.

It is relevant to notice that if muon neutrinos oscillate into tau neutrinos, as atmospheric neutrino experiment results suggest (Ambrosio 1998a; Fukuda et al. 1999), ν_τ are subject to considerably less absorption than muon neutrinos (Halzen & Saltzberg 1998; Bottai & Becattini 1999). Tau neutrinos are subject to a regeneration effect in the Earth: ν_τ interacts and the produced tau lepton immediately decays with negligible energy loss; hence from τ decay another ν_τ is produced. This effect, more noticeable for harder spectra, has been neglected here.

The fluxes of detectable upward-going muons for sources with $\gamma = 2.1$ and $\delta = -60°$,0° are shown as a function of muon energy with and without absorption in Figure 8. If one assumes that the normalization of the neutrino flux is of the order of the upper limits from gamma-ray experiments at $\sim$100 TeV (2×10^{-13} cm^{-2} s^{-1} for the Galactic center), the expected rate of neutrino-induced muons varies between 10^{-2} and 10^{-3} (10^{-1} and 10^{-2}) events yr^{-1} 1000 m^{-2} for $\gamma = 2.1$ (2.5), depending on the declination of the source. Note that the softer the source spectrum, the higher the neutrino event rates.

An important quantity in the search for celestial point sources is the effective angular spread of the detected muons with respect to the neutrino direction. We have computed the angle between the neutrino and the detected muon using a Monte Carlo simulation. We have assumed a neutrino flux of the form $dN/dE_\nu = \text{constant} \times E^{-\gamma}$ for several neutrino spectral indices γ and considered the neutrino cross sections, the muon energy loss in the rock, and the detector angular resolution. Table 2 shows the fraction of the events in a 3° search half-cone for two different spectral indices as a function of the zenith angle. With the simulations of monoenergetic muon beams on a box larger than the detector, including $\sim$2 m of rock, we have calculated the effective

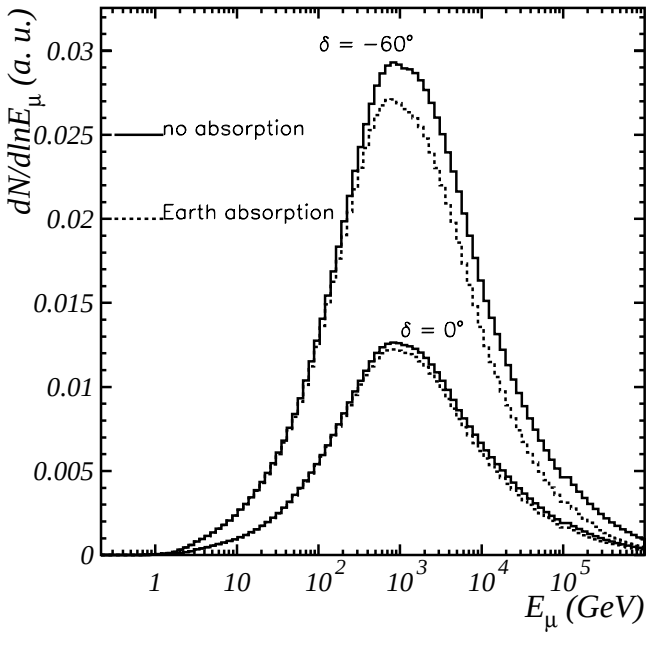

FIG. 8.—Differential rate of detected muons as a function of muon energy in MACRO for spectral indices $\gamma = 2.1$ and for sources at declinations $-60°$ and 0° with (*dotted line*) and without (*solid line*) absorption.

TABLE 2

FRACTION OF EVENTS INSIDE A CONE OF 3° HALF-WIDTH FOR TWO SPECTRAL INDICES AND FOR FIVE ZENITH ANGLES

$\cos\theta$	$\gamma = 2$	$\gamma = 2.2$
0.15.....	0.77	0.72
0.55.....	0.91	0.87
0.75.....	0.91	0.87
0.95.....	0.91	0.87

area and even checked that our intrinsic resolution does not worsen with energy due to the effect of increasing electromagnetic showers induced by stochastic energy losses of muons. Up to 100 TeV, the average angle between the generated muons and the reconstructed ones is less than 1°.

5. SEARCH FOR POINTLIKE SOURCES

The MACRO data sample is shown in equatorial coordinates (right ascension in hours and declination in degrees) in Figure 9. For the pointlike source search using the direction information of upward-going muons, we evaluate the background due to atmospheric neutrino-induced muons by randomly mixing 100 times the local angles of upward-going events with their times. The number of mixings is chosen to have a statistical error for the background about 10 times smaller than the data fluctuations. The local angles are then smeared by $\pm 10°$ in order to avoid repetitions, particularly in the declination regions where there is small acceptance. The value of 10° is chosen to have variations larger than the dimensions of the search cones.

For a known candidate pointlike source S, the background in the search cone $\Delta\Omega = \pi\omega^2$, with ω the half-width of the search cone in radians, is evaluated by counting the events in a declination band around the source declination δ_S of $\Delta\delta = \pm 5°$:

$$N_{\rm back} = \frac{N(\Delta\delta)\Delta\Omega}{2\pi[\sin(\delta_S + 5°) - \sin(\delta_S - 5°)]} . \quad (9)$$

We have considered the case of a possible detection of an unknown source represented by an excess of events clustered inside cones of half-widths 1.°5, 3°, and 5°. Hence we have looked at the number of events falling inside these cones around the direction of each of the 1100 measured events. The cumulative result of this search is shown in Figure 10 for the data (*filled circles*) and the simulation of atmospheric events (*solid line*). We find 60 clusters of four or more muons around a given muon (including the event itself), to be compared with 56.3 expected from the background of atmospheric neutrino-induced muons. The largest cluster is made of seven events in the 3° half-cone, and it is located around the equatorial coordinates (right ascension, declination) = (222.°5, −72.°7). Two other clusters of six events in 3° are located around (188.°1, −48.°1) and (342.°5, −74.°4), respectively. Nevertheless, they are not statistically significant with respect to atmospheric neutrino background.

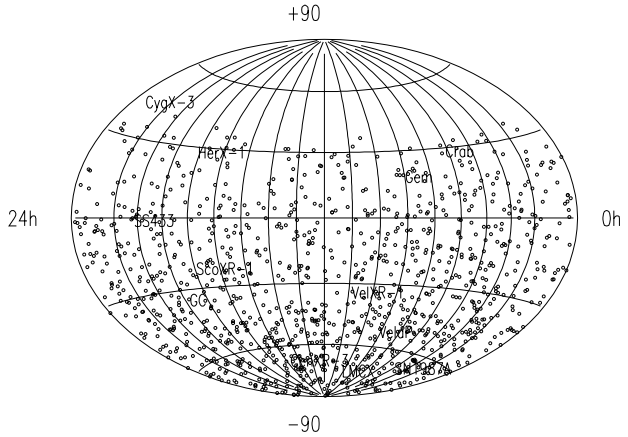

FIG. 9.—Upward-going muon distribution in equatorial coordinates (1100 events).

For our search among known point sources, we have considered several existing catalogs: the recent EGRET catalog;[32] a catalog of BL Lacertae objects (Padovani & Giommi 1995), of which 181 fall in the visible sky of MACRO ($-90° \le \delta \lesssim 50°$); the list of eight sources in the visible sky emitting photons above tera–electron volts already mentioned in § 1; the Green catalog[36] of SNRs; the BATSE catalogs;[33] 32 *BeppoSAX* GRBs (E. Pian 1999, private communication); and a compilation of 29 novae X (N. Masetti 1999, private communication), which are binaries with a compact object and a companion star that transfers mass into an accretion disk. Novae X are characterized by sudden increases of luminosities in the X range ($L \sim 10^{37}$–10^{38} ergs s^{-1} reached after 20–90 days). From these catalogs, we have selected 42 sources we consider interesting because they have the features required by the "beam dump" model. In Figure 11 the distribution of the numbers of events falling in the search cones is shown for the data and the simulation for the 42 sources. We find no statistically significant excess from any of the considered sources with respect to the atmospheric neutrino background. For the 42 selected sources, we find 11 sources with two or more events in a search cone of 3°, to be compared to 12.0 sources expected from the simulation.

Upper limits on muon fluxes from sources can be calculated at a given confidence level, e.g., 90% c.l., as

$$\Phi\ (90\%\ \text{c.l.}) = \frac{\text{upper limit (90\% c.l.)}}{\text{effective area} \times \text{live time}} , \quad (10)$$

where the numerator is the upper limit calculated from the number of measured events and from the number of expected background events and the denominator is the exposure of the detector, which is the area of the apparatus seen by the source during its running time. Different methods to evaluate upper limits are described in Caso et al. (1998). We have calculated the upper limits (the numerator in eq. [10]) using the recent and well-motivated unified approach by Feldman & Cousins (1998). The 90% c.l. muon and neutrino flux limits are given in Table 3 for the 42 selected sources. These limits are valid for muon energies greater than 1 GeV. They include the effect of the absorption of muon neutrinos in their propagation through the Earth. The limits are obtained assuming a neutrino spectrum from a source with $\gamma = 2.1$. Moreover, the effect of the decrease in efficiency at very high energies and the reduction factors for a search half-cone of 3° and a spectral

[36] Green, D. A. 1998, A Catalog of Galactic Supernova Remnants, available at the URL http://www.mrao.cam.ac.uk/surveys/snrs.

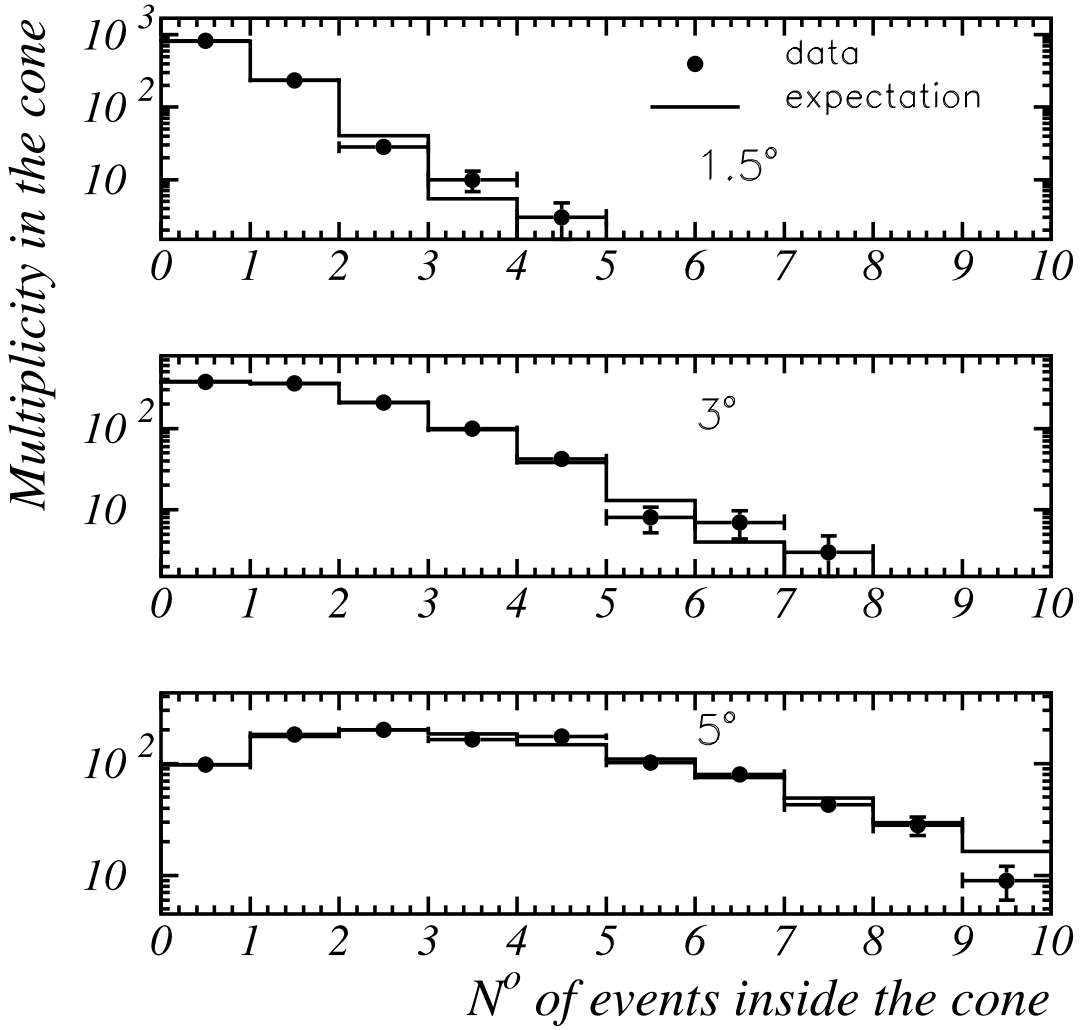

FIG. 10.—On the x-axis there are the number of events falling in cones of half-width 1°.5, 3°, and 5° (*from top to bottom plots*) around the direction of any muon. The y-axis depends on the total number of events considered. *Filled circles*: data. *Solid line*: simulation.

index $\gamma = 2.1$ (given in Table 2) are included. For comparison we include the best limits from previous experiments. In order to see how the limits depend on the spectral index γ, we report in Table 4 the percentage difference of the exposure as a function of declination calculated for a source with $\gamma = 2.1$ and a source with $\gamma = 2.3, 2.5, 2.7$, and 3.7.

We have calculated the neutrino flux upper limits in the last column of Table 3 from muon flux upper limits. As can be seen in equation (7), the muon and neutrino upper limits are related one to the other. We calculate upper limits assuming a neutrino flux with power-law spectrum with $\gamma = 2.1$, integrating neutrino energies from 1 GeV. The inferred neutrino upper limits are strongly model dependent, while muon upper limits are not.

As we mention in § 2, the neutrino spectrum resulting from sources in which p-γ scattering dominates is almost constant with energy below a threshold (Berezinsky & Gazizov 1993). At energies larger than this threshold, the spectrum follows the primary spectrum power law. If this threshold is reached at large values of neutrino energy, the calculated neutrino upper limits would differ by orders of magnitude from the ones calculated for a power-law spectrum resulting from p-p scattering because the two spectra are different in a wide energy range. Most of the models involving p-γ scattering for AGNs (Szabo & Protheroe 1994) predict neutrino spectra which follow the proton spectrum down to low energies when protons remain confined in the central region by the turbulent magnetic fields necessary for the diffusive shock acceleration to work (Gaisser et al. 1995). Other models, such as Stecker et al. (1991), in which protons are not confined at the source, predict a neutrino spectrum which follows the proton spectrum only down to an energy threshold of roughly 500 TeV. In the case of the Stecker et al. flatter spectrum, the MACRO response curve has a maximum at energies around $\sim 10^3$ TeV (while for a power-law spectrum with $\gamma = 2.1$, the maximum is between 10 and 20 TeV, as shown in Fig. 6). The resulting neutrino upper limit in the cases of Mrk 421 and Mrk 501 is larger by a factor of $\sim 4 \times 10^3$ than the one for $\gamma = 2.1$.

To evaluate the physical implications of our limits on muon fluxes, we recall that a muon flux of the order of 0.03×10^{-14} cm^{-2} s^{-1} is expected from the supernova remnant Vela Pulsar (Gaisser 1996), which predicts a yield of neutrinos at the level of about 1 order of magnitude lower than present limits.

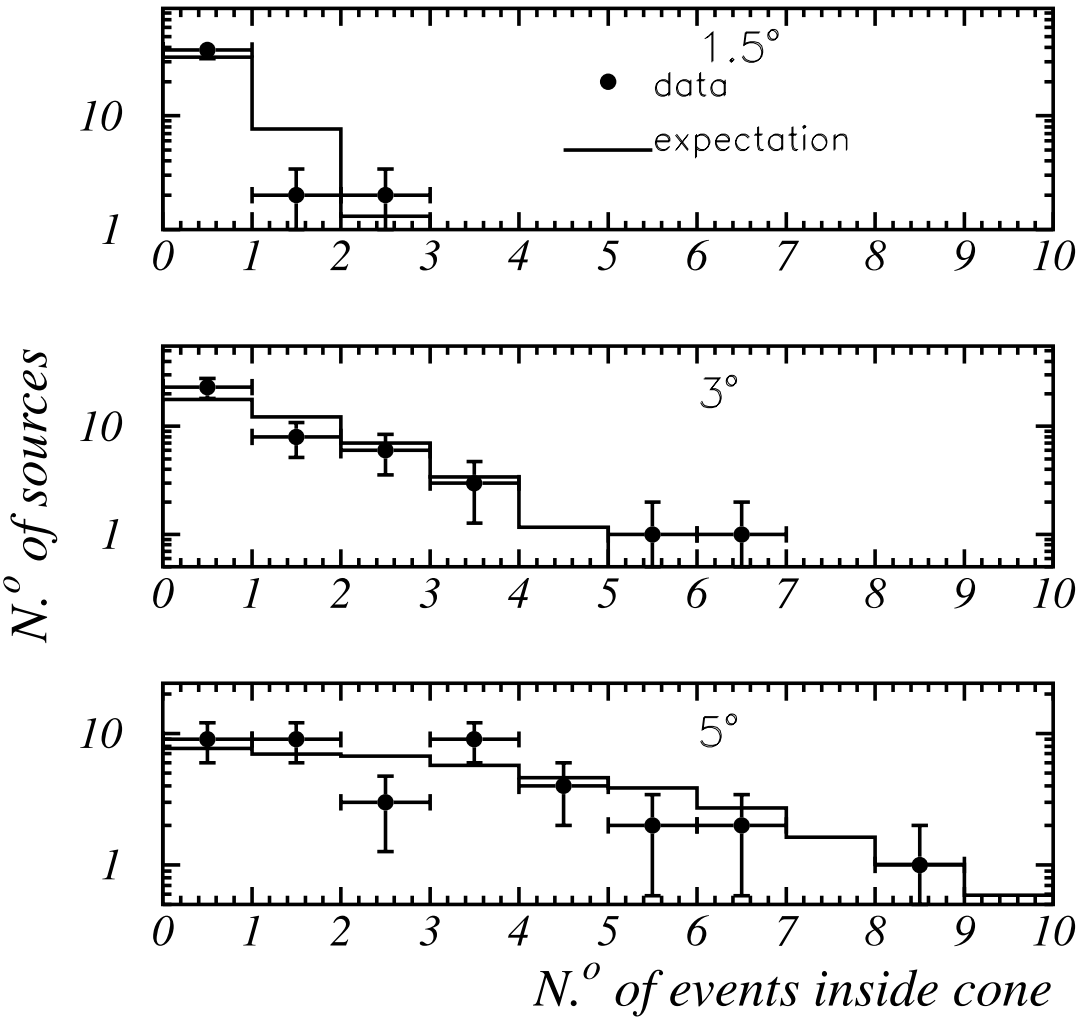

FIG. 11.—On the x-axis there are the number of events falling in cones of half-width 1°.5, 3°, and 5° (*from top to bottom*) around the direction of the 42 sources considered. The y-axis depends on the total number of sources considered. *Filled circles*: data. *Solid line*: simulation.

We notice that there are six events from GX 339−4 in a 3° search cone with chance probability $P = 6 \times 10^{-3}$. Considering that we have looked at 42 sources, the probability of finding such an excess from at least one of these sources is 8.6% (evaluated from Fig. 11).

Between the selected 42 candidate sources, Mrk 421 and Mrk 501 are particularly interesting due to the strong emissions (in the tera–electron volt region) they present. These emissions have variable intensity over time. Mrk 421 shows a strongly variable emission, with peak flares during 1995 June, 1996 May, and 1998 April (Krennrich et al. 1999). Mrk 501 had a high state of emission during about 6 months in 1997, particularly intense between April and September (Protheroe et al. 1997). The strongest flare in 1998 occurred on March 5. Unfortunately, the MACRO exposure for these sources is not favored because they are seen almost at the horizon, where the acceptance is lower. No event from both sources is found inside a search cone as large as 5°. Only two events for each of the sources are found inside 10°. They are of marginal interest due to the large angle with respect to the source directions. They have been measured in periods in which there were no known intense flares (for Mrk 421: 1996 September 10 and 1998 June 27; for Mrk 501: 1996 September 29 and 1998 June 26).

We have also made a search for neutrino signals using a cumulative analysis: for each of several catalogs of source types, we set a limit on the flux from sources from that catalog. In some situations (e.g., for a uniform distribution in the space of sources having the same intensity), this method could give a better sensitivity than the search for a single source. It depends on the spatial distribution and on the intensity of the sources.

We consider the average value N_0 of the distribution for the data and the average value N_B of the distribution for the simulation in Figure 11 for the 42 sources in the MACRO list, in Figure 12 for the 220 SNRs, in Figure 13 for the 181 blazars, and in analogous plots for the other catalogs. Then we estimate the cumulative upper limits for N sources in the catalog as

$$\Phi_{\text{cumulative}}\ (90\%\ \text{c.l.}) = \frac{\text{upper limit (90\% c.l.)}}{\text{average area} \times \text{live time}}\,, \qquad (11)$$

where the average area is $[\sum_{i=1}^{N} \text{Area}(\delta_i)]/N$, with $\text{Area}(\delta_i)$ the area seen by a source with declination δ_i. The upper

TABLE 3

90% CONFIDENCE LEVEL NEUTRINO-INDUCED MUON FLUX LIMITS FOR THE MACRO LIST OF 42 SOURCES

Source	δ (deg)	Events in 3°	Background in 3°	ν-Induced μ-Flux Limits (10^{-14} cm^{-2} s^{-1})	Previous Best μ-Limits (10^{-14} cm^{-2} s^{-1})	ν-Flux Limits (10^{-6} cm^{-2} s^{-1})
SMC X-1	−73.5	3	2.1	0.62	...	1.18
LMC X-2	−72.0	0	2.0	0.15	...	0.33
LMC X-4	−69.5	0	2.0	0.15	0.36 B	0.29
SN 1987A	−69.3	0	2.0	0.15	1.15 B	0.31
GX 301−2	−62.7	2	1.8	0.53	...	1.10
Cen X-5	−62.2	2	1.7	0.55	...	1.04
GX 304−1	−61.6	2	1.7	0.54	...	1.05
Cen XR-3	−60.6	1	1.7	0.36	0.98 I	0.68
Cir XR-1	−57.1	5	1.7	1.18	...	2.21
2U 1637−53	−53.4	0	1.7	0.19	...	0.36
MX 1608−53	−52.4	0	1.7	0.20	...	0.38
GX 339−4	−48.8	6	1.7	1.62	...	3.00
Ara XR-1	−45.6	3	1.6	1.00	...	1.87
Vela Pulsar	−45.2	1	1.5	0.51	0.78 I	0.94
GX 346−7	−44.5	0	1.5	0.23	...	0.43
SN 1006	−41.7	1	1.3	0.56	...	1.04
Vela XR-1	−40.5	0	1.3	0.26	0.45 B	0.55
2U 1700−37	−37.8	1	1.3	0.58	...	1.08
L10	−37.0	2	1.1	0.91	...	1.72
Sgr XR-4	−30.4	0	0.9	0.34	...	0.63
Galactic center	−28.9	0	0.9	0.34	0.95 B	0.65
GX 1+4	−24.7	0	0.9	0.36	...	0.67
Kep 1604	−21.5	2	0.9	1.12	...	2.12
GX 9+9	−17.0	0	0.9	0.40	...	0.75
Sco XR-1	−15.6	1	0.9	0.85	1.5 B	1.59
Aqr	−1.0	4	0.8	2.48	...	4.66
4U 0336+01	0.6	1	0.8	1.17	...	2.19
Aql XR-1	0.6	0	0.8	0.57	...	1.18
2U 1907+2	1.3	0	0.8	0.58	...	1.27
Ser XR-1	5.0	0	0.7	0.67	...	1.41
SS 433	5.7	0	0.7	0.67	1.8 B	1.27
2U 0613+09	9.1	1	0.6	1.52	...	3.02
Geminga	18.3	0	0.5	1.12	3.1 I	2.10
Crab	22.0	1	0.4	2.52	2.6 B	4.70
2U 0352+30	31.0	2	0.3	5.98	...	11.43
Cyg XR-1	35.2	0	0.2	3.24	...	6.24
Her X-1	35.4	0	0.2	3.30	4.3 I	6.96
Cyg XR-2	38.3	0	0.1	4.99	...	10.61
Mrk 421	38.4	0	0.1	5.00	3.3 I	9.56
Mrk 501	40.3	0	0.1	5.73	...	10.69
Cyg X-3	40.9	0	0.1	6.59	4.1 I	12.49
Per XR-1	41.5	0	0.1	7.51	...	13.99

NOTES.—Corresponding limits on the neutrino flux are given in the last column for $E_{\nu\min} = 1$ GeV. These limits are calculated for $\gamma = 2.1$ and for $E_\mu > 1$ GeV, including the decrease in efficiency at very high energies. The reduction factors for a 3° half-width cone are included. These limits include the effect of absorption of neutrinos in the Earth. The flux upper limits are calculated with the unified approach of Feldman & Cousins 1998. "B" indicates the results of Baksan (Boliev et al. 1995); "I" the results of IMB (Svoboda et al. 1987; Becker-Szendy 1995a, 1995b).

limit is evaluated for $N_0 > N_B$ as

$$\text{upper limit (90\% c.l.)} = N_0 - N_B + 1.28(\text{rms}/\sqrt{N}) , \quad (12)$$

where rms is the root mean square value of the considered expected distributions, and for $N_0 < N_B$ as

$$\text{upper limit (90\% c.l.)} = 1.28(\text{rms}/\sqrt{N}) . \quad (13)$$

We obtain $\Phi_{\text{lim}}(90\%) = 3.06 \times 10^{-16}$ cm^{-2} s^{-1} for the 42 sources in the MACRO list. This can be considered a limit on a diffuse flux.

In the case of the 220 SNRs in the Green catalog, we obtain the cumulative upper limit from the cumulative analysis shown in Figure 12 of 2.63×10^{-16} cm^{-2} s^{-1}. This can be considered a diffuse muon flux limit for neutrino production from supernova remnants. For the 181 blazars in Padovani & Giommi (1995; see Fig. 13), we find a cumulative upper limit of the muon flux 5.44×10^{-16} cm^{-2} s^{-1}. In Table 5 we summarize the upper limits for the various catalogs considered.

Finally, it is interesting to note that most of the models for neutralino annihilation in the Galactic center in Gondolo & Silk (1999) are excluded by our experimental upper limit of $\sim 3 \times 10^{-15}$ cm^{-2} s^{-1} when there is a central spike for a 3° cone. In Table 6 the muon flux limits (90% c.l.) for various search cones around the direction of the Galactic center (3°, 5°, and 10°) for five values of the neutralino mass from 60 GeV to 1 TeV are calculated. The dependence of the effective area of the detector as a function of the neutrino energy has been calculated folding with the neutrino flux from neutralino annihilation calculated by

TABLE 4

PERCENTAGE INCREASE (+) OR DECREASE (−) OF MACRO EXPOSURE

δ (deg)	Difference (%) $\gamma = 2.3$	Difference (%) $\gamma = 2.5$	Difference (%) $\gamma = 2.7$	Difference (%) $\gamma = 3.7$
−90.....	+4.1	+5.9	+5.2	−23.8
−80.....	+2.8	+4.2	+3.9	−18.7
−70.....	+3.0	+4.6	+4.5	−18.7
−60.....	+2.9	+4.5	+4.4	−18.9
−50.....	+2.7	+4.0	+3.6	−19.9
−40.....	+3.0	+4.6	+4.4	−18.6
−30.....	+3.0	+4.5	+4.2	−19.0
−20.....	+3.0	+4.4	+3.9	−20.0
−10.....	+3.3	+4.9	+4.4	−20.4
0.....	+3.7	+5.6	+5.3	−19.5
10	+3.8	+5.8	+5.7	−19.5
20	+4.1	+6.6	+7.1	−15.8
30	+5.1	+7.8	+7.8	−17.2
40	+5.0	+7.4	+6.9	−16.7

NOTE.—Increase or decrease of exposure is between a source producing a neutrino spectrum with $\gamma = 2.3$, 2.5, 2.7 (such as in the case of atmospheric neutrinos with $E_\nu \lesssim 10$ GeV), and 3.7 (such as in the case of high-energy atmospheric neutrinos) with respect to the $\gamma = 2.1$ spectrum.

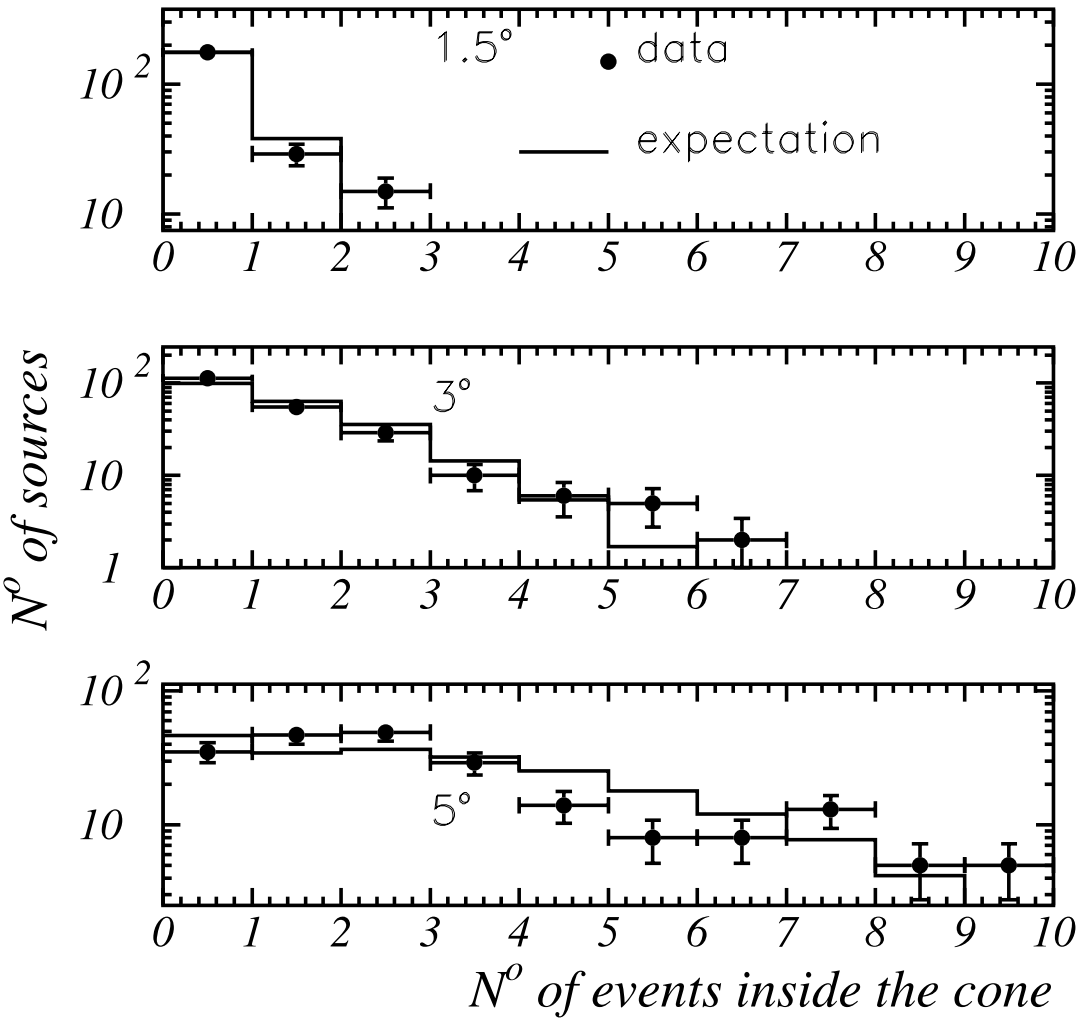

FIG. 12.—On the x-axis there are the number of events falling in cones of half-width 1°.5, 3°, and 5° (*from top to bottom*) around the direction of 220 SNRs from Green catalog (see footnote 34 in text). The y-axis depends on the total number of sources considered. *Filled circles*: data. *Solid line*: simulation.

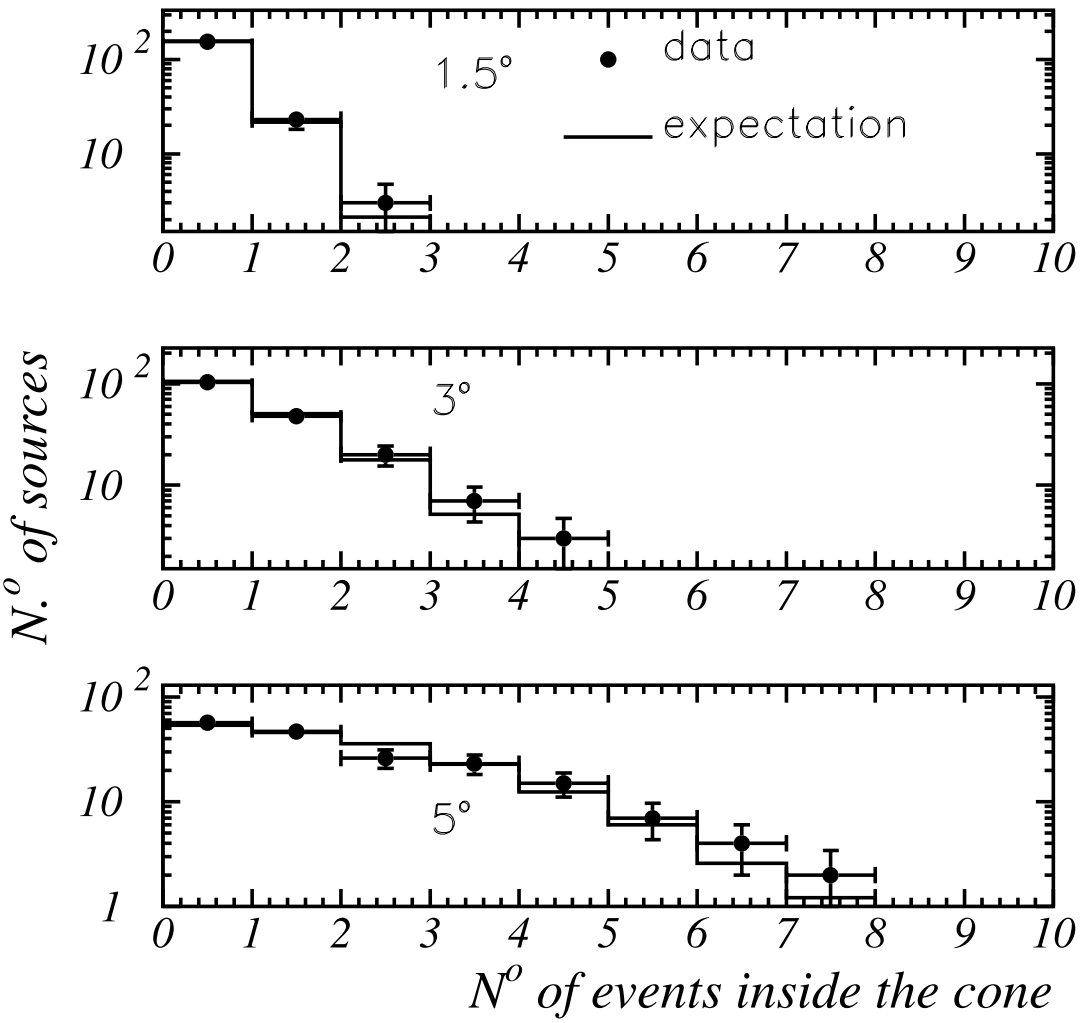

FIG. 13.—On the x-axis there are the number of events falling in cones of 1°.5, 3°, and 5° around the direction of 181 blazars from Padovani & Giommi (1995). The y-axis depends on the total number of sources considered. *Filled circles*: data. *Solid line*: simulation.

Bottino et al. (1995). As a first approximation, the difference of using the neutrino fluxes by Gondolo & Silk (1999) in the effective area calculation should be negligible. The limits are calculated for $E_\mu > 1$ GeV.

6. SEARCH FOR CORRELATIONS WITH GAMMA-RAY BURSTS

We look for correlations with the gamma-ray bursts given in the BATSE Catalogs 3B and 4B,[33] containing 2527

TABLE 5

FLUX UPPER LIMITS ON MUON FLUXES FROM NEUTRINO PRODUCTION FROM VARIOUS CATALOGS

Catalog	Number of Sources	Average Exposure ($\times 10^{-14}$ cm^{-2} s^{-1})	ν-Induced μ-Flux Limit ($\times 10^{-16}$ cm^{-2} s^{-1})	ν-Flux Limit (cm^{-2} s^{-1})
MACRO list	42	4.67	3.06	5.79×10^{-8}
SNRs (Green catalog)[a]	220	2.35	2.63	5.00×10^{-8}
Blazars (Padovani & Giommi 1995)	181	2.77	5.44	1.03×10^{-7}
BATSE[b]	2527	3.37	1.68	3.17×10^{-8}
EGRET[c]	271	3.66	2.03	3.82×10^{-8}
BeppoSAX (E. Pian 1999, private communication)	32	3.41	6.84	1.27×10^{-7}
Novae X (N. Masetti 1999, private communication)	29	4.97	5.34	1.01×10^{-7}

NOTE.—Flux upper limits are at 90% c.l. for $E_\mu > 1$ GeV and for an assumed spectral index of the neutrino flux of $\gamma = 2.1$. The catalog, the number of souces in it, the average exposure (which is the denominator in eq. [11]), the muon flux upper limits, and the neutrino flux upper limits ($E_{\nu\min} = 1$ GeV) are given. Flux upper limits are calculated according to eqs. (12) and (13).

[a] Green, D. A. 1998, A Catalog of Galactic Supernova Remnants, available at the URL http://www.mrao.cam.ac.uk/surveys/snrs.

[b] Paciesas, W. S., et al. 1999, available at the URL http://gammaray.msfc.nasa.gov/batse.

[c] Hartman, R. C., et al. 1998, available at the URL ftp://gamma.gsfc.nasa.gov/pub/THIRD_CATALOG.

TABLE 6

90% Confidence Level Upper Limits on Upward Muon Fluxes Induced by Neutrinos from Annihilation of Neutralinos Trapped in the Galactic Center

Cone (deg)	Data	Background	μ-Flux Limits ($\times 10^{-15}$ cm^{-2} s^{-1})				
			$m_\chi = 60$ GeV	$m_\chi = 100$ GeV	$m_\chi = 200$ GeV	$m_\chi = 500$ GeV	$m_\chi = 1000$ GeV
3	0	0.9	3.67	3.42	3.26	3.21	3.21
5	1	2.6	4.70	4.37	4.17	4.11	4.11
10.....	10	10.3	13.66	12.71	12.11	11.96	11.94

Notes.—For neutralino masses $m_\chi = 60$, 100, 200, 500, and 1000 GeV and various search cones around its direction. These limits are for $E_\mu > 1$ GeV, and upper limits are calculated according to Feldman & Cousins 1998. These limits constrain strongly the model by Gondolo & Silk 1999; compare to their Fig. 3.

gamma-ray bursts from 1991 April 21 to 1999 October 5. They overlap in time with 1085 upward-going muons collected by MACRO during this period. The effective area for upward-going muon detection in the direction of the bursts averaged over all the bursts in the catalog is 121 m^2. Its value is small because our detector is sensitive to neutrinos only in one hemisphere and because it was not complete in the period 1991–1994. Figure 14 shows our neutrino events and BATSE GRBs as a function of the year.

We find no statistically significant correlation between neutrino events and gamma-burst directions for search cones of 10°, 5°, and 3° half-widths. The width of the search cones is related to the BATSE angular resolution; these cones include 96.9%, 85.1%, and 70.5% neutrinos, respectively, if emitted from GRBs. These numbers do not include the contributions due to the muon neutrino angle, to the muon propagation in the rock, or to the MACRO angular resolution, which are small with respect to BATSE angular resolution.

We also consider possible time correlations between MACRO and BATSE events. For the temporal coincidences, we use both the position information and the time information. In order to calculate the background we add 200 temporal shifts to the time difference between the event detected by other experiments and the ν event in MACRO, considering various time intervals (the minimum interval is [−4000 s, 4000 s], the maximum interval is [−80,000 s, 80,000 s]). We consider time windows of ±400 s every 20 s.

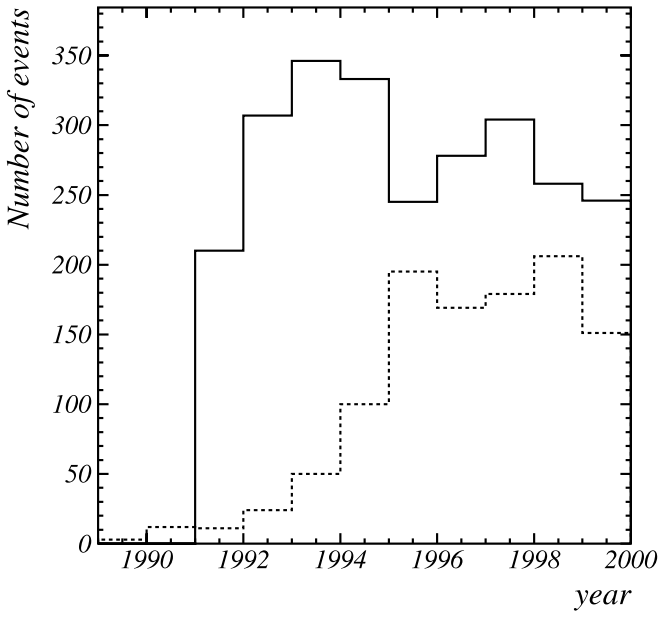

Fig. 14.—MACRO events (*dashed line*) and BATSE GRBs (*solid line*) as a function of year.

We find one event after 39.4 s from the 4B 950922 gamma-ray burst of 1995 September 22 at an angular distance of 17°.6 and another very horizontal event in coincidence with the 4B940527 gamma-ray burst of 1994 May 27 inside 280 s at 14°.9. The 90% c.l. muon flux limit is calculated for a search cone of 10° around the gamma-burst direction and in an arbitrary time window of ±200 s. The choice of this time window is arbitrary because one does not know a priori what the duration of the neutrino emission is. Models of GRB emitters are not yet clear in predicting when and for how long neutrinos are emitted. This is in fact the reason why we have considered even a directional analysis of GRBs using no time information (see previous section). On the other hand, in this section we are using the time information, and our choice of the time window where we set the upper limit is motivated only by the fact that this window is larger than the duration of 97.5% of the 3B Catalog GRBs (for which the measured durations are available). In the chosen search window we find no events to be compared to 0.04 expected background events. Figure 15 shows the difference in time between the detection of an upward-going muon and a GRB as a function of the cosine of their angular separation. Two scales are shown: the upper plot is an expanded scale of the lower one.

The corresponding flux upper limit (90% c.l.) is 0.79×10^{-9} cm^{-2} upward-going muons per average burst. The limit is almost 8 orders of magnitude lower than the flux coming from an "extreme" topological defect model reported in Halzen & Jaczo (1996), while according to a model in the context of the fireball scenario (Waxman & Bahcall 1997), a burst at a distance of 100 Mpc producing 0.4×10^{51} ergs in neutrinos of about 10^{14} eV would produce $\sim 6 \times 10^{-11}$ cm^{-2} upward-going muons.

The same analysis on space and time correlations has been performed for 32 *BeppoSAX* events; the result is compatible with the atmospheric neutrino background.

7. CONCLUSIONS

We have investigated the possibility that the sample of 1100 upward-going muons detected by MACRO since 1989 shows evidence of a possible neutrino astrophysics source. We do not find any significant signal with respect to the statistical fluctuations of the background due to atmospheric neutrinos from any of the event directions or from any

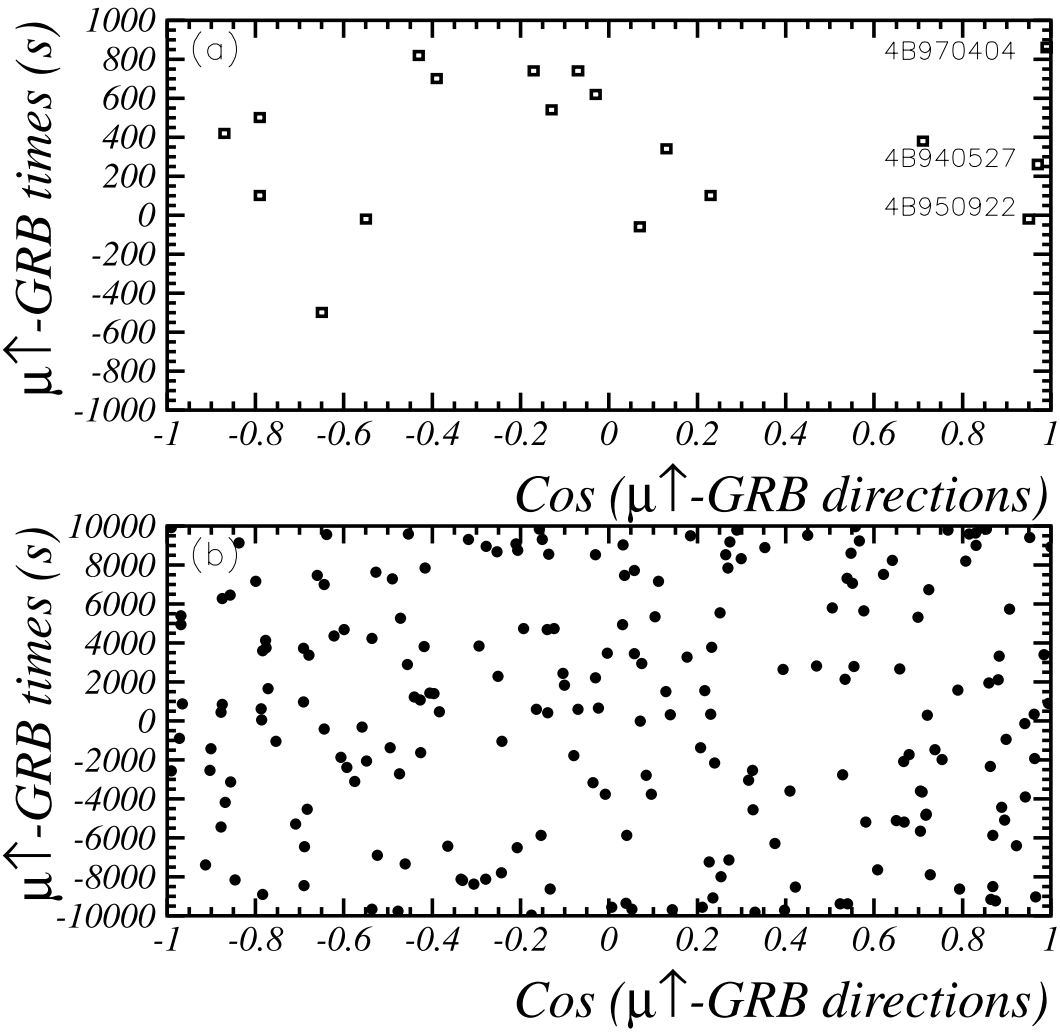

FIG. 15.—Difference in detection times vs. the cosine of the angular separation between MACRO upward-going muon events and BATSE gamma-ray bursts. Panels *a* and *b* have different timescales. The BATSE GRB of 1995 September 22 (4B 950922) was detected 39.4 s before one MACRO event at an angular distance of 17°.6 and the BATSE (4B 940527) GRB of 1994 May 27 280 s after another very horizontal MACRO event at 14°.9. In *a* they are indicated with the name of the bursts.

candidate sources. We also used the time information to look for correlations with gamma-ray bursts detected by BATSE and *BeppoSAX*. Having found no excess of events with respect to the expected background, we set muon and neutrino flux upper limits for pointlike sources and for the cumulative search of catalogs of sources. These limits have been calculated taking into account the response of MACRO to various neutrino fluxes from candidate sources up to energies $\gtrsim 100$ TeV. These limits are for almost all of the considered sources the most stringent ones compared to other current experiments. They are about 1 order of magnitude higher than values quoted by most plausible neutrino source models except for the model in Gondolo & Silk (1999), which is seriously constrained.

We gratefully acknowledge the support of the director and of the staff of the Laboratori Nazionali del Gran Sasso and the invaluable assistance of the technical staff of the institutions participating in the experiment. We thank the Istituto Nazionale di Fisica Nucleare (INFN), the US Department of Energy, and the US National Science Foundation for their generous support of the MACRO experiment. We thank INFN, ICTP (Trieste), and NATO for providing fellowships and grants for non-Italian citizens.

REFERENCES

Adarkar, H., et al. (KGF Collaboration). 1991, ApJ, 380, 235
———. 1995, in Proc. 24th Int. Cosmic-Ray Conf. (Roma), 1, 820
Ahlen, S. P., et al. (MACRO Collaboration). 1993, Nucl. Instrum. Methods Phys. Res., A324, 337
Ambrosio, M., et al. (MACRO Collaboration). 1995, Phys. Lett., B357, 481
———.1998a, Phys. Lett., B434, 451
———. 1998b, Astropart. Phys., 9, 105
———.1999, Phys. Rev. D, 59, 012003
Bahcall, J. N., & Frautschi, S. C. 1964, Phys. Rev., 135, 788
Balkanov, V. A., et al. 2000, in Beyond the Desert 99: 2d Int. Conf. on Particle Physics Beyond the Standard Model, ed. I. V. Krivosheina & H. V. Klapdor-Kleingrothaus (Bristol: Institute of Physics), 1053
Becker-Szendy, R., et al. 1995a, ApJ, 444, 415
———. 1995b, Nucl. Phys. B, 38, 331
Berezinsky, V. S., Castagnoli, C., & Galeotti, P. 1985, Nuovo Cimento, 8C, 185
Berezinsky, V. S., & Gazizov, A. Z. 1993, Phys. Rev. D, 47, 4206
Bionta, R. M., et al. 1987, Phys. Rev. Lett., 58, 1494

Boliev, M. M., et al. (Baksan Collaboration). 1995, in Proc. 24th Int. Cosmic-Ray Conf. (Roma), 1, 722
Bottai, S., & Becattini, F. 1999, in Proc. 26th Int. Cosmic-Ray Conf. (Salt Lake City), 2, 249
Bottai, S., & Perrone, L. 2000, preprint (hep-ex/0001018)
Bottino, A., Fornengo, N., Mignola, G., & Moscoso, L. 1995, Astropart. Phys., 3, 65
Brun, R., et al. 1987, CERN Report DD/EE/84-1
Caso, C., et al. 1998, Rev. Part. Phys. (European Phys. J.), C3, 1
Chadwick, P. M., et al. 1999, ApJ, 513, 161
Corona, A., et al. (MACRO Collaboration). 1995, in Proc. 24th Int. Cosmic-Ray Conf. (Roma), 1, 800
Costa, E., et al. 1997, IAU Circ. 6576
Davis, R., Jr., Harmer, D. S., & Hoffman, K. C. 1968, Phys. Rev. Lett., 20, 1205
Feldman, G. J., & Cousins, R. D. 1998, Phys. Rev. D, 57, 3873
Frontera, F. 1997, in Proc. 25th Int. Cosmic-Ray Conf. (Durban), 8, 307
Fukuda, Y., et al. (Super-Kamiokande Collaboration). 1999, Phys. Rev. Lett., 82, 2644
Gaisser, T. K. 1996, Nucl. Phys. B, 48, 405
Gaisser, T. K., Halzen, F., & Stanev, T. 1995, Phys. Rep., 258, 173
Gandhi, R., Quigg, C., Reno, M. H., & Sarcevic, I. 1996, Astropart. Phys., 5, 81
———. 1998, Phys. Rev. D, 58, 093009
Gondolo, P., & Silk, J. 1999, Phys. Rev. Lett., 83, 1719
Greisen, K. 1960, Annu. Rev. Nucl. Sci., 10, 1
———. 1966, Phys. Rev. Lett., 16, 748
Halzen, F. 2000, in Neutrinos in Physics and Astrophysics: From 10^{-33} to 10^{28} cm, ed. P. Langacker (Singapore: World Scientific), 524
Halzen, F., & Hooper, D. W. 1999, ApJ, 527, L93
Halzen, F., & Jaczo, G. 1996, Phys. Rev. D, 54, 2779
Halzen, F., & Saltzberg, D. 1998, Phys. Rev. Lett., 81, 4305
Hirata, K., et al. 1987, Phys. Rev. Lett., 58, 1490
Jackson, J. D., Gove, H. E., & Lüth, V. 1993, Annu. Rev. Nucl. Part. Sci., 43, 883
John, K., et al. (AMANDA Collaboration). 1999, in Proc. 26th Int. Cosmic-Ray Conf. (Salt Lake City), 2, 196
Kifune, T., et al. 1995, ApJ, 438, L91
Krennrich, F., et al. 1999, in Proc. 26th Int. Cosmic-Ray Conf. (Salt Lake City), 3, 301
Lai, H., et al. (CTEQ Collaboration). 1995, Phys. Rev. D, 51, 4763
Lang, M. J., et al. 1990, Nucl. Phys. A, 14, 165
Lohmann, W., Kopp, R., & Voss, R. 1985, CERN Yellow Report CERN 85-03
Longair, M. S. 1997, High Energy Astrophysics, Vol. 1 (2d ed., repr. with corrections; Cambridge: Cambridge Univ. Press)
Mannheim, K., Protheroe, R. J., & Rachen, J. P. 1998, Phys. Rev. D, submitted (astro-ph/9812398)
Metzger, M. R., et al. 1997, Nature, 387, 878
Oyama, Y., et al. 1989, Phys. Rev. D, 39, 1481
Padovani, P., & Giommi, P. 1995, MNRAS, 277, 1477
Petry, D., et al. 1997, in Proc. 25th Int. Cosmic-Ray Conf. (Durban), 3, 241
Piran, T. 1999, Phys. Rep., 314, 575
Plothow-Besch, H. 1993, Comput. Phys. Commun., 75, 396
Protheroe, R. J., Bednarek, W., & Luo, Q. 1998, Astropart. Phys., 9, 1
Protheroe, R. J., et al. 1997, in Proc. 25th Int. Cosmic-Ray Conf. (Durban), 8, 317
Punch, M., et al. 1992, Nature, 358, 477
Quinn, J., et al. 1996, ApJ, 456, L83
Rachen, J. P., & Meszaros, P. 1998, Phys. Rev. D, 58, 123005
Rhode, W., et al. (Frejus Collaboration). 1996, Astropart. Phys., 4, 217
Sako, T., et al. 1997, in Proc. 25th Int. Cosmic-Ray Conf. (Durban), 3, 193
Sigl, G., Lee, S., Schramm, D. N., & Coppi, P. 1997, Phys. Lett., B392, 129
Stecker, F. W., Done, C., Salamon, M. H., & Sommers, P. 1991, Phys. Rev. Lett., 66, 2697 (erratum 69, 2738 [1992])
Svoboda, R., et al. (IMB Collaboration). 1987, ApJ, 315, 420
Szabo, A. P., & Protheroe, R. J. 1994, Astropart. Phys., 2, 375
Tanimori, T., et al. 1998, ApJ, 497, L25
Vietri, M. 1998, Phys. Rev. Lett., 80, 3690
Waxman, E., & Bahcall, J.N. 1997, Phys. Rev. Lett., 78, 2292
———. 1999, Phys. Rev. D, 59, 023002 (WB)
Wolf, G. 1995, Nucl. Phys. B, 38, 107
Yoshikoshi, T., et al. 1997, ApJ, 487, L65
Zatsepin, G. T., & Kuz'min, V. A. 1966, Pisma Zh. Eksp. Teor. Fiz., 4, 114